E949:

An experiment to measure the branching ratio $\mathbf{B}(K^+ \to \pi^+ \nu\overline{\nu})$

March 1999

Contents

List of Tables

List of Figures

E949
An experiment to measure the branching ratio $B(K^+ \to \pi^+ \nu\overline{\nu})$

M.S. Atiya[(2)], E.W. Blackmore[(8)], P.C. Bergbusch[(8)], D.A. Bryman[(8)], S. Chen[(8)], I-H. Chiang[(2)], M.V. Diwan[(2)], J.S. Frank[(2)], J.S. Haggerty[(2)], M.P. Grigoriev[(6)] T. Inagaki[(5)], A.P. Ivashkin[(6)], V. Jain[(2)], S. Kabe[(5)], S.H. Kettell[(2)], M.M. Khabibullin[(6)], A.N. Khotjantsev[(6)], P. Kitching[(1)], M. Kobayashi[(5)], T.K. Komatsubara[(4)], A. Konaka[(8)], Y.G. Kudenko[(6)], Y. Kuno[(5)], T.F. Kycia[(2)], K.K. Li[(2)], L.S. Littenberg[(2)], J.A. Macdonald[(8)], J. Mildenberger[(8)], O.V. Mineev[(6)], M. Miyajima[(3)], N. Muramatsu[(4)], T. Nakano[(7)], H.-S. Ng[(1)], J. Nishide[(3)], M. Nomachi[(7)], T. Numao[(8)], K. Omata[(4)], J.-M. Poutissou[(8)], R. Poutissou[(8)], G. Redlinger[(8)], T. Sato[(5)], K. Shimada[(3)], T. Shinkawa[(5)], T. Shimoyama[(3)], R.C. Strand[(2)], S. Sugimoto[(4)], Y. Tamagawa[(3)], Y. Yoshimura[(5)], and C. Witzig[(2)].

[(1)]Centre for Subatomic Research, University of Alberta, Edmonton, Alberta T6G 2N5, Canada
[(2)]Brookhaven National Laboratory (BNL), Upton, NY 11973, United States
[(3)]Fukui University, Bunkyo, Fukui 910-8507, Japan
[(4)]High Energy Accelerator Research Organization (KEK), Tanashi branch, Midori, Tanashi, Tokyo 188-8501, Japan
[(5)]High Energy Accelerator Research Organization (KEK), Oho, Tsukuba, Ibaraki 305-0801, Japan
[(6)]Institute for Nuclear Research RAS, 60 October Revolution Pr. 7a, 117312 Moscow, Russia
[(7)]Research Center for Nuclear Physics, Osaka University, Mihogaoka, Ibaraki, Osaka 567-0047, Japan
[(8)]TRIUMF, 4004 Wesbrook Mall, Vancouver, B.C. V6T 2A3, Canada

beam: LESB3, low energy (600-800 MeV/c) separated K^+ beam. The beam conditions are expected to be a 730 MeV/c K^+ beam with a K^+/π^+ ratio of >3:1 with 65 Tp on the C-target. The expected spill length is ~4.1 sec and a Duty Factor of 64%.

detector: Solenoidal magnetic spectrometer, with 4π calorimetric detection of all decay products except neutrinos.

hours: Request 6,000 hours. This should represent 2 years of running in the RHIC era. Expect to be ready for data collection during the fall of 2000.

spokespersons: Douglas Bryman, doug@triumf.ca, (604)222-7338.
Steve Kettell, kettell@bnl.gov, (516)344-5323.
Shojiro Sugimoto, shojiro.sugimoto@kek.jp, (+81)424-69-9548.

Abstract

A new, more precise measurement of the $K^+ \to \pi^+ \nu\overline{\nu}$ branching ratio is proposed. Improvements to the E787 apparatus and running mode will be made to reach a sensitivity of $(8\text{–}15)\times10^{-12}$, an order of magnitude below the Standard Model prediction. This will result in a determination of $|V_{td}|$ to better than 30%.

Executive Summary

A new, more precise measurement of the $K^+ \to \pi^+ \nu\overline{\nu}$ branching ratio is proposed. This experiment, E949, was given the highest rating by the BNL High Energy and Nuclear Physics Program Advisory Committee. Improvements to the E787 apparatus and modifications to the Alternating Gradient Synchrotron (AGS) operating mode will be made to reach a sensitivity of $(8\text{–}15)\times 10^{-12}$, an order of magnitude below the Standard Model (SM) prediction of $\sim 1 \times 10^{-10}$. This will result in a determination of $|V_{td}|$ to better than 30%.

Experiment E787 presented evidence for this decay based on the observation of a clean event from data collected in the 1995 run of the AGS. The expected level of background was 0.08 events. The branching ratio indicated by this observation, $\mathrm{B}(K^+ \to \pi^+ \nu\overline{\nu}) = 4.2^{+9.7}_{-3.5} \times 10^{-10}$, is consistent with the SM expectation although the central experimental value is four times larger. The final sensitivity is expected to reach below 10^{-10}. The apparently large branching ratio, along with the surprisingly large value of ϵ'/ϵ give additional impetus for E949 to extend further and more fully explore the possibility of new physics, or alternatively to make a precise measurement of $|V_{td}|$.

The intrinsic theoretical uncertainty of determining $|V_{td}|$ from a measurement of $\mathrm{B}(K^+ \to \pi^+ \nu\overline{\nu})$ is small (<6%). This decay, combined with the neutral analog $K^\circ_L \to \pi^\circ \nu\overline{\nu}$, provides the cleanest, most accurate determination of the CKM unitarity triangle parameters $\overline{\rho}$ and $\overline{\eta}$. In order to confront the Standard Model explanation for CP violation, determination of these parameters from the K system is essential. Such measurements are complementary to those obtained from the B system and any discrepancy between the values found in the K and B systems would be a strong indicator of new physics.

Since E949 uses the same technique as E787, the extensive experience in data analysis provides a high level of confidence in projecting the sensitivity of E949. A low energy K^+ beam is stopped in an active, segmented target. Backgrounds are rejected by precise, redundant measurements of the decay π^+ kinematics, by identification of the particle as a π^+ , and by vetoing of any other particle associated with the K^+ decay. The momentum, energy and range of the decay π^+ are measured in a low mass drift chamber and a segmented plastic scintillator range stack. The π^+ is positively identified by observation of the $\pi^+ \to \mu^+ \to e^+$ decay chain. Photons, or any other particles associated with the K^+ decay are vetoed by a nearly 4π photon veto system.

E787 was primarily limited by the number of AGS protons available. The backgrounds were sufficiently small for a background-free measurement of the branching ratio, even if it is substantially smaller than that predicted by the Standard Model.

The E949 experiment plans to use 5–7 times more protons per spill than E787. This increase in proton flux will be used to increase the number of stopped kaons without significant loss in acceptance. Since there is a loss in acceptance as rates in the detector increase, the experimental sensitivity will be increased by reducing the kaon momentum, thereby increasing the fraction of kaons that stop, and by increasing the duty factor of the AGS. Although many of the improvements in E949 arise by increasing the sensitivity without increasing the rates in the detector, there will also be a number of improvements to the detector to decrease background and increase acceptance.

The increased sensitivity of E949 is achieved by a combination of several factors:

- An increased number of protons per spill on the kaon production target (C-target). The E787 experiment typically ran with less than 15 Tp/spill (Tp = 10^{12} protons) during 1995–97; E949 will run at 65 Tp/spill.
- The increased flux of protons will be used in part to lengthen the AGS spill. E949 will gain in sensitivity with the increase in the AGS duty factor.
- The K^+ beam from the increased flux of protons will be used at lower momentum where the fraction of kaons that stop in the segmented target increases.
- Detector improvements will increase live time and acceptance. The data size and readout deadtime will be reduced by adding a TDC system to the range stack counters, allowing the readout region for the 500 MHz transient digitizers to be reduced. The first level trigger deadtime will be reduced by pipelining and improved electronics. The accidental losses from online photon vetos will be reduced through meantiming.
- The data taking efficiency of the experiment will be increased. Real-time monitoring of several key systems will be implemented. Additional spare modules will be made for several critical electronics components. Additional diagnostics will be written for facilitating a rapid diagnosis of data acquisition problems.
- E949 will take advantage of the longer running periods available during Relativistic Heavy Ion Collider (RHIC) operation ($\geq$25 weeks/year symbiotic with RHIC).
- The photon veto system will be enhanced with a barrel veto liner and additional detectors along the beam line. The beam counters will be more finely segmented, establishing a tighter spatial correlation of the incident kaon with the kaon position in the target. The target will be augmented with a new position-measuring system to enhance pattern recognition efficiency. The light yield of the trigger counters will be increased, increasing their efficiency. The electronics of the drift chamber will be modified to enhance the track reconstruction efficiency.
- Improvements to the data acquisition system will allow the experiment to run at higher throughput.

This important contribution to the understanding of the CKM matrix element $|V_{td}|$ and the origin of CP-violation in the Standard Model can be realized with a modest investment from DOE. The capital request from DOE for the necessary maintenance of and improvements to the detector and beamline is \$1.8 M (\$FY00). An additional in-kind contribution of \$1.8 M derived from Canadian, Japanese and Russian collaborators has been confirmed. The E949 collaboration consists of Brookhaven National Laboratory, TRIUMF, the University of Alberta, KEK, Fukui University, RCNP at Osaka University, and INR–Moscow.

1 Introduction

The E787 experiment has presented evidence for the $K^+ \to \pi^+\nu\overline{\nu}$ decay based on the observation of a clean event from data collected in the 1995 run of the AGS. The branching ratio indicated by this observation is consistent with the Standard Model expectation although the central experimental value exceeds it by a factor of four.

This rare decay, a flavor changing neutral current process, first arises at the one loop level[1] in the Standard Model. The presence of the top quark in the loops[2] makes this decay very sensitive to the modulus of the elusive CKM coupling V_{td} [3]. Moreover, this sensitivity can be fully exploited because of the hard GIM suppression, the relatively small QCD corrections which have been calculated to next-to-leading-logarithmic order[4–6], and the fact that the normally problematic hadronic matrix element can be determined to a few percent from the rate of K_{e3} ($K^+ \to \pi^\circ e^+\nu_e$) decay. In fact, corrections to the latter have now been calculated, reducing this uncertainty even further[7]. Even the main higher order electroweak corrections have been shown to be very small[8]. Taking account of all known contributions to the intrinsic theoretical uncertainty, the branching ratio can be calculated to 7%[3] given the SM input parameters such as $|V_{td}|$. Conversely, if B($K^+ \to \pi^+\nu\overline{\nu}$), m_t, $|V_{cb}|$, etc., were well known, $|V_{td}|$, could be determined to <6%. QCD corrections to the charm contribution are the leading source of the residual theoretical uncertainty.

Although in principle, long-distance contributions could spoil the connection between the branching ratio B($K^+ \to \pi^+\nu\overline{\nu}$) and $|V_{td}|$, a number of calculations have shown them to be negligible[9–13]. This implies that not only can the effects of SM short-distance physics be clearly discerned in this process, but also the effects of possible non-SM physics. Most forms of new physics postulated to augment or supersede the SM have implications for B($K^+ \to \pi^+\nu\overline{\nu}$)[14]. Recently, attention has focussed on the possible effects of a fourth generation[15], leptoquarks[16–18], a left-right symmetric model[19], technicolor[20,21], various forms of supersymmetry[22–29] and assorted others[30–32]. It is notable that the effects of SUSY upon the K and B system almost always turn out to be discernibly different. This also tends to be true for other possible new physics. Very recently the surprisingly large value of ϵ'/ϵ reported by the KTeV group[33] has excited speculation that new physics may be at work in the K system. In a large number of models (*e.g.* supersymmetric ones), the same interactions that have the potential to raise ϵ'/ϵ, can have large effects on $K^+ \to \pi^+\nu\overline{\nu}$. For example in the usual application of supersymmetry to flavor changing neutral currents, the reported central value of ϵ'/ϵ with its error can accommodate a value of B($K^+ \to \pi^+\nu\overline{\nu}$) as large as 3.5×10^{-10}[34,35], very close to E787's initial branching ratio!

In the SM, using current data on m_t, m_c, V_{cb}, $|V_{ub}/V_{cb}|$, ϵ_K, B°—$\overline{B^\circ}$ mixing, etc., the branching ratio is expected to be B($K^+ \to \pi^+\nu\overline{\nu}$) = (0.6–1.5)$\times 10^{-10}$[36]. If the latest experimental input and theoretical calculations are fit, scanning each parameter within the range of its estimated error, Buchalla and Buras[6] obtain a more precise prediction of B($K^+ \to \pi^+\nu\overline{\nu}$) = $(0.82 \pm 0.32) \times 10^{-10}$. A measurement of B($K^+ \to \pi^+\nu\overline{\nu}$) along with that for the neutral analog B($K_L^\circ \to \pi^\circ\nu\overline{\nu}$) completely determines the CKM triangle[1] (see Fig. 1). Measurements of these decays are the

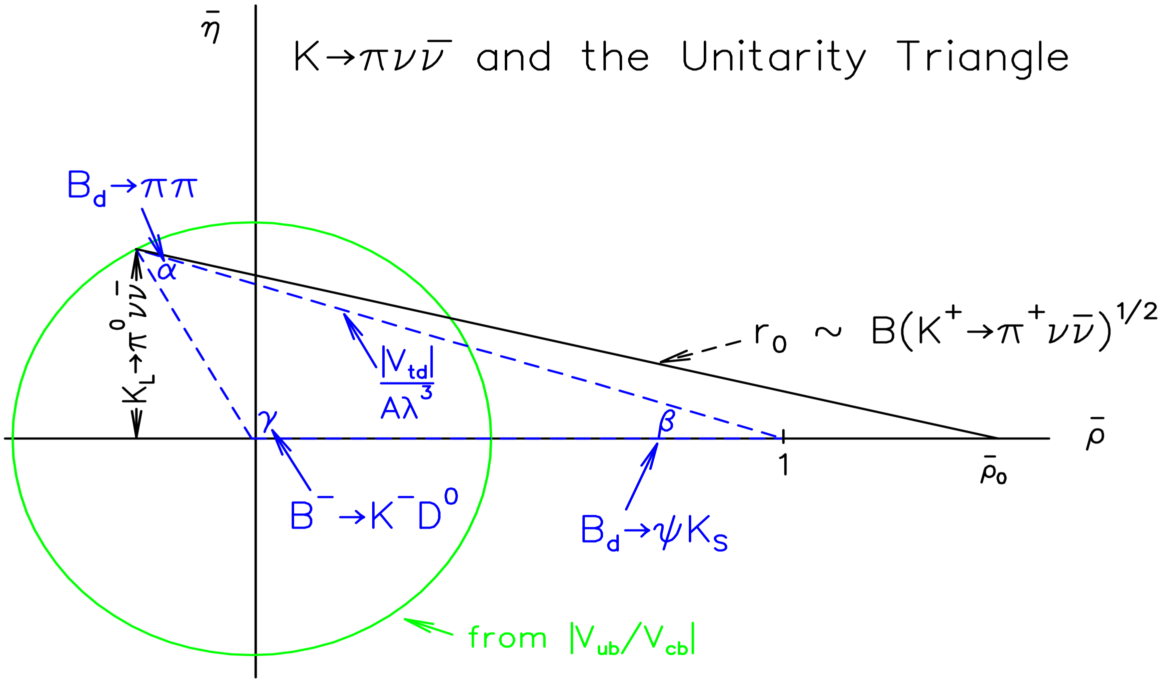

Figure 1: CKM triangle determination from the K and B systems.

theoretically cleanest ways of determining the CKM parameters $\overline{\rho}$ and $\overline{\eta}$[36]. In order to confront the Standard Model explanation for CP violation, determination of these parameters from the K system is essential. Such measurements are complementary to those obtained from the B system and any discrepancy in the values found would be a strong indicator of new physics.

The E787 experiment is expected to reach a single event sensitivity (S.E.S.) below 10^{-10} from data acquired through 1998. Although there is a large statistical uncertainty in the current determination of the branching ratio, if the central value holds up, several additional events will be seen and new physics would be indicated. To fully explore this possibility or to to make a precise measurement of $|V_{td}|$ assuming the SM level for $K^+\to\pi^+\nu\overline{\nu}$, the new measurement proposed here will obtain a single event sensitivity of (8–15)$\times10^{-12}$, an order of magnitude below the SM prediction.

2 Results from E787

The E787 experiment had its first significant running period during the 1989–91 runs of the AGS. The experiment and beam line underwent a major upgrade from 1992–94, and took data from 1995–98.

[1]This assumes that m_t and $|V_{cb}|$ are known.

2.1 Evidence for $K^+ \to \pi^+ \nu\overline{\nu}$

The first observation of the $K^+ \to \pi^+ \nu\overline{\nu}$ decay[37] was based on data from the 1995 run of E787. The range and energy of event candidates passing all other cuts is shown in Fig. 2. The box indicates the signal region. One event consistent with

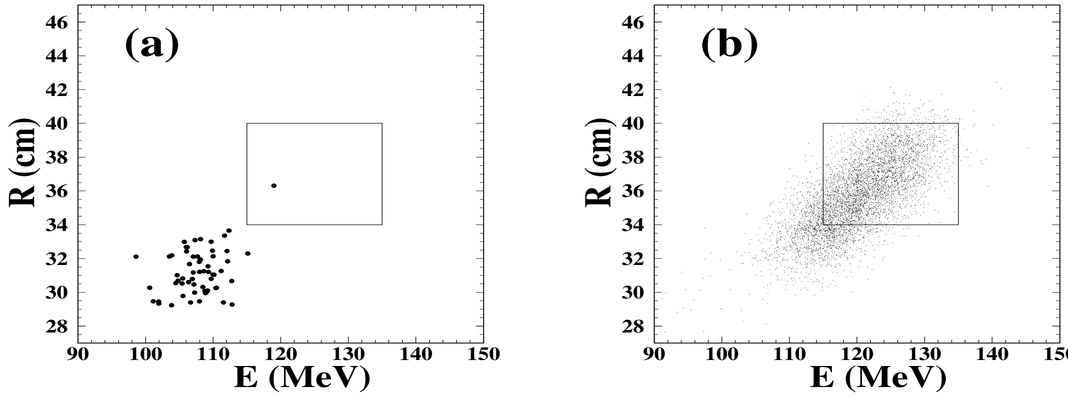

Figure 2: Final event candidate for $K^+ \to \pi^+ \nu\overline{\nu}$: a) Data b) Monte-Carlo

the decay $K^+ \to \pi^+ \nu\overline{\nu}$ was observed. The measured background from all sources was 0.08 ± 0.03 events (equivalent to a branching ratio of 3×10^{-11}). This event was in a particularly clean region where the expected background was 0.008 ± 0.005 and which contained 55% of the acceptance of the full signal region. A reconstruction of the event is shown in Fig. 3. The kaon decayed to a pion at 23.9 ns, followed by a clean $\pi^+ \to \mu^+$ decay 27.0 ns later, as can be seen in the upper insert in Fig. 3; there was a clean $\mu^+ \to e^+$ decay 3201.1 ns later. There was no significant activity anywhere else in the detector at the time of the K^+ decay. The branching ratio for $K^+ \to \pi^+ \nu\overline{\nu}$ implied

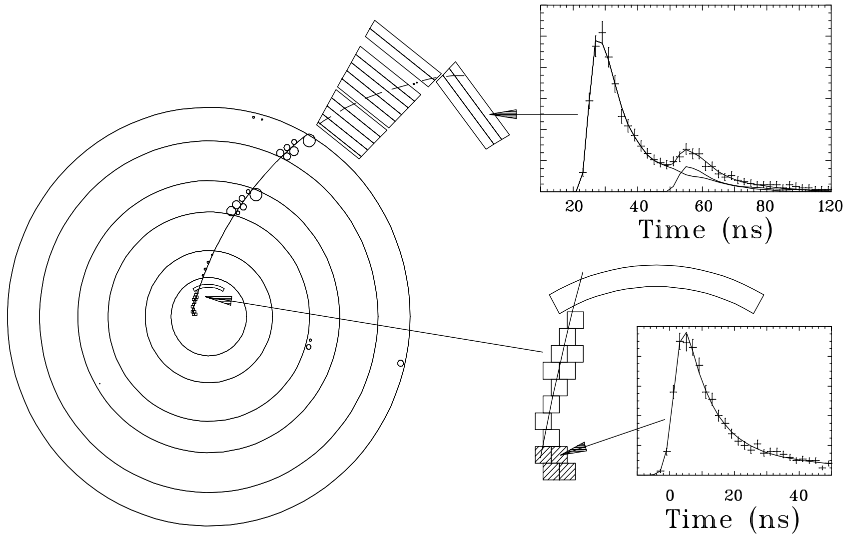

Figure 3: $K^+ \to \pi^+ \nu\overline{\nu}$ event.

by the observation of this event is $B(K^+ \to \pi^+ \nu\overline{\nu}) = 4.2^{+9.7}_{-3.5} \times 10^{-10}$.

2.2 E787 Data

The expected sensitivity from the data already on tape (1995–98) is 5 times that of the 1995 data alone. Improved analysis software has demonstrated a background rejection on the 1995–97 data set that is more than a factor of 2 larger, with comparable acceptance. This level of background (equivalent to a branching ratio of 10^{-11}) is sufficient for E949. Results of analyzing this larger data set are expected shortly.

Typical conditions during the 1995 run included 13 Tp/spill, 5.3 MHz of incident K^+ , a stopped kaon rate of 1.2 M/spill, a deadtime of 25%, an online photon veto loss of 10% and an acceptance of 0.16%. This acceptance is 60% of the acceptance at zero rate. The rates in most detector elements were proportional to the incident flux rather than the stopped kaon flux. This implies that E949 can substantially increase sensitivity by increasing the fraction of stopped kaons/incident kaons, as will be discussed in Section 3 below.

2.3 $K^+ \to \pi^+ \nu\overline{\nu}$ below the $K^+ \to \pi^+\pi^\circ$ peak

The published 1995 result was obtained from $K^+ \to \pi^+ \nu\overline{\nu}$ with a π^+ momentum above the $K^+ \to \pi^+\pi^\circ$ ($K_{\pi 2}$) peak at 205 MeV/c. The region below the $K_{\pi 2}$ peak has been deemphasized in the primary search for the decay $K^+ \to \pi^+ \nu\overline{\nu}$ because of the low momentum tail of $K_{\pi 2}$ decays resulting from pion-nucleus interactions. However, this momentum region has attractive prospects for the study of $K^+ \to \pi^+ \nu\overline{\nu}$. It has more phase space and suffers less from pion absorption because slower pions are further from the $\Delta(1236)$ resonance. These factors can increase the acceptance up to a factor of 3 times larger than that above the $K_{\pi 2}$ peak. Also, if non-SM physics were present, the π^+ momentum spectrum could be drastically different; for the case of scalar couplings[39], the maximum of the spectrum occurs around 150 MeV/c, instead of at the endpoint (227 MeV/c).

Using 1989 data, the published upper limit for the region below the $K_{\pi 2}$ was 1.7×10^{-8} (90% C.L.)[38] based on no candidate events. The most serious background comes from $K_{\pi 2}$ decays, where the π^+ loses energy in nuclear interactions and the detector fails to detect either of the two photons from the π° decay.

With the 1992–94 upgrade of the detector, the photon veto capability was enhanced at least by a factor of three and the detection efficiency of extra energy or a visible kink in the target track (indicating nuclear interaction) was significantly improved. Moreover π/μ identification was improved by three orders of magnitude due to the better momentum resolution and demultiplexed range stack scintillators. At present, the analysis of 1995–97 data is in progress in parallel to the analysis of the region above the $K_{\pi 2}$ peak. The expected sensitivity from the 1995–97 data is at the level of the SM prediction with the same level of background.

3 Overview of E949

The E787 detector[40] is the foundation for the new experiment. E949 was given the highest rating by the BNL High Energy and Nuclear Physics Program Advisory

Committee. Since E949 uses the same technique as E787, that extensive experience in data analysis provides a high level of confidence in projecting the sensitivity of E949.

The detection of $K^+ \to \pi^+ \nu\overline{\nu}$, a single incident K^+ followed by the decay to a single π^+ of momentum $P < 227$ MeV$/c$ and no other observable products, requires suppression of all backgrounds to well below the sensitivity for the signal, preferably to the level of 10^{-11}. The two most significant backgrounds are the two body decays $K^+ \to \mu^+ \nu_\mu$ ($K_{\mu 2}$, with BR=64%) and $K^+ \to \pi^+ \pi^\circ$ (BR=21%). The $K^+ \to \pi^+ \nu\overline{\nu}$ signal can be observed in the region away from these two kinematic peaks. A plot of the momentum spectra of the π^+ from $K^+ \to \pi^+ \nu\overline{\nu}$ is shown in Fig. 4. The

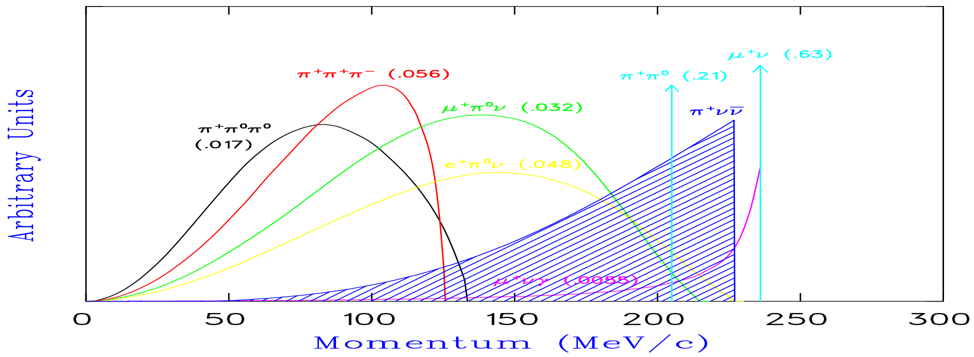

Figure 4: Momentum in the center of mass of charged particles from the major K^+ decay modes and $K^+ \to \pi^+ \nu\overline{\nu}$. (Branching ratios in parentheses.)

only other significant background comes from either a π^+ in the beam scattering into the detector or from K^+ charge exchange.

The three sets of tools for suppressing backgrounds are redundant measurements of particle kinematics (momentum, energy and range), particle identification and photon vetoing. The $K_{\mu 2}$ is rejected by particle identification, for not having a $\pi^+ \to \mu^+ \to e^+$ decay chain and by its mono-energetic decay. The $K_{\pi 2}$ is rejected by detecting one of the two photons from the π° decay as well as by its mono-energetic decay. The scattered pions are rejected by good particle identification in the beam, tracking of both the kaon and the pion, and requiring that the putative kaon decay at rest in the target (by requiring that the π^+ track occur later than the incident K^+ track). The charge exchange background, from a $K^+ + n \to p + K^\circ$ interaction followed by $K^\circ_L \to \pi^+ \ell^- \overline{\nu_\ell}$, is rejected by identification of the extra particles (the proton and charged lepton) and by the delayed coincidence. To satisfy the delayed coincidence, the $K^\circ_{\rm L}$ has to remain in the target without decaying for at least 2 ns. The cross section for these slow $K^\circ_{\rm L}$'s is measured to be very small.

The primary improvement for E949 is stopping more K^+ near the center of the detector, without significantly increasing the instantaneous rates in the detector. At significantly higher flux from the AGS, the increased duty factor and lowered kaon momentum leave the instantaneous rate of incident kaons essentially unchanged. At lower kaon momentum the fraction of kaons that stop increases, so the sensitivity increases (e.g. for a constant flux of incident kaons, the acceptance is constant and the sensitivity increases at the lower momentum). Additional improvement arises from the longer running time envisioned while the AGS is serving as an injector into RHIC and from increased trigger, data acquisition (DAQ) and running efficiency. Upgrades to the E787 detector and DAQ are needed to increase the background rejection in the region below the $K_{\pi 2}$ peak and to increase the DAQ bandwidth for the increased sensitivity.

3.1 The E949 Detector

A drawing of the E787 detector upgraded for this experiment is shown in Fig. 5. The detector is located in the C4 beam line at the AGS. The C4 beam line, or Low

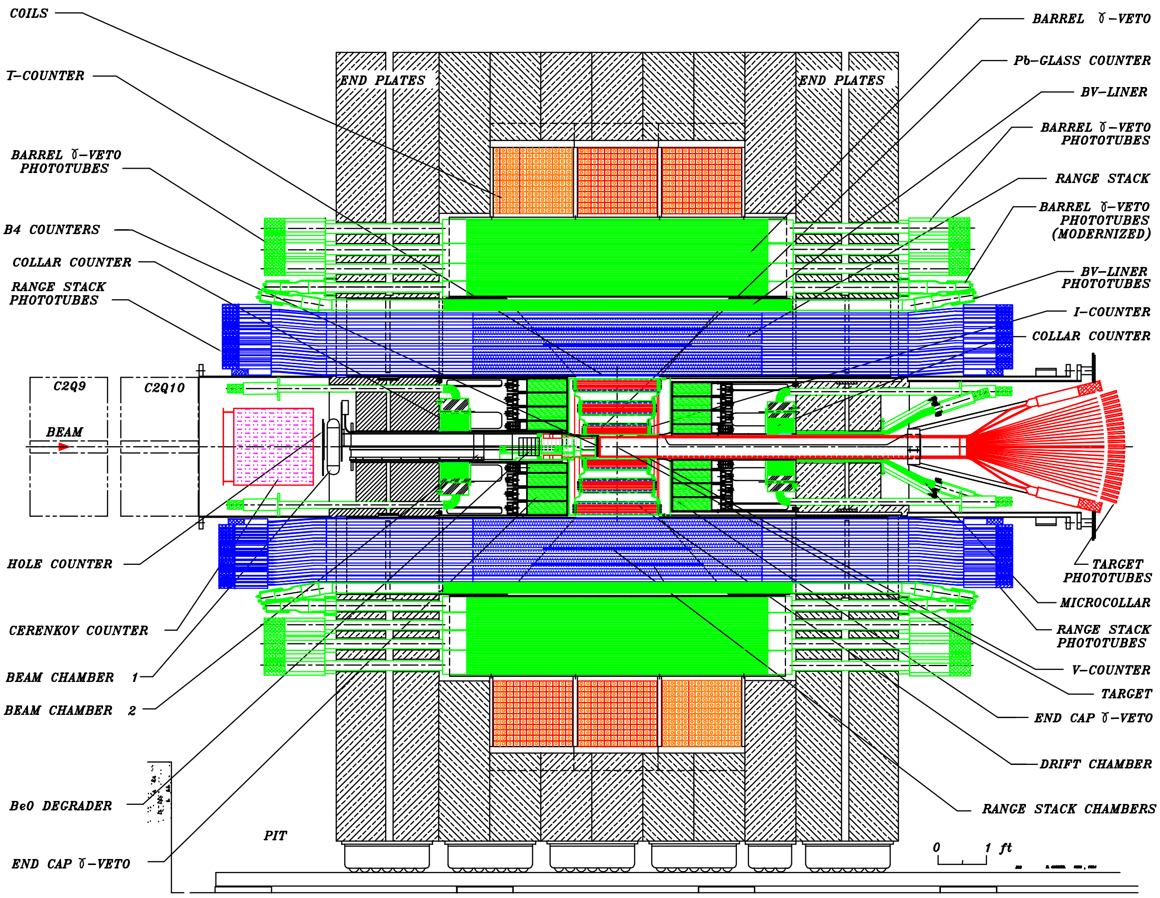

Figure 5: The E949 detector.

Energy Separated Beam (LESB3)[41], transports kaons of up to 830 MeV/c. At 690 MeV/c it can transmit more than $3 \times 10^6 K^+$/spill with a K^+/π^+ ratio of 3:1 for 10^{13} protons on the production target. The K^+ are stopped in a scintillating fiber target in the center of the detector. The detector, which for vetoing purposes is hermetic, is located in a 1 T, solenoidal magnetic field.

The incident kaons are identified in a Cherenkov counter, two tracking counters and then, after slowing down in an active degrader, an energy loss (dE/dx) counter before coming to rest in the central target.

The scintillating fiber target (TT) consists of 413 5-mm square fibers. Each fiber is 310 cm long and read out by a single PMT. The K^+ , incident along the length of the fibers typically hits only a few fibers, but deposits substantial energy in each. The outgoing π^+ typically hits several fibers and deposits $\sim$1 MeV in each. The target's high light output and low level of dead material provides good energy and timing information on both the incident K^+ and outgoing π^+ . The target is surrounded by 272 smaller scintillating fibers read out by 16 PMTs and by 6 scintillators (IC), whose 24.1 cm length determines the fiducial region of the target.

The central drift chamber[42] (UTC) is a cylindrical, low-mass chamber that consists of 12 layers of axial wire cells and six layers of thin cathode strip foils supported by differential gas pressure. The chamber is arranged in three super-layers: each super-layer consists of four layers of axial sense wires in a square cell arrangement and two layers of thin foils with helical Cu cathode strips. The induced charge on the cathode strips, which are tilted at 45° to the z-axis, is used to determine the longitudinal(z) coordinate. A track is expected to have 12 xy and 6 z measurements. The momentum resolution for muons and pions in the range 150–250 MeV/c is <1% and the z-resolution is <1 mm. The chamber has 20 μm Au-plated tungsten sense wires and 100 μm Al field shaping wires. The chamber runs with a 50:50 mix of argon-ethane, with N_2 between the super-layers. The total amount of material in the active momentum measuring section of chamber is 2×10^{-3} radiation lengths ($X_\circ$).

The energy, range, and decay sequence of charged particles are measured in the range stack (RS). They are stopped in this cylindrical array of 19 layers and 24 azimuthal sectors of plastic scintillator. Each counter is read out with a PMT on each end. The innermost layer, 24 T-counters, are 0.52 m long to define the acceptance and 6.35 mm thick. The remaining layers, 2–18, are 1.82 m long and 19.05 mm thick. The final layer, 19, is 1 cm thick. Two layers of straw tube detectors (RSSC) are located after layers 10 and 14, to provide fine resolution tracking within the RS.

Fig. 6 shows the resolution of one set of kinematic variables for pions and muons selected with particle identification cuts.

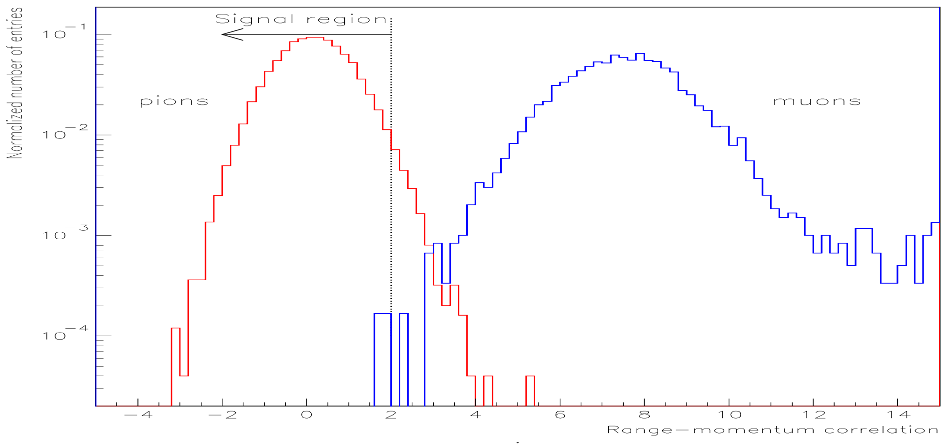

Figure 6: Kinematic separation of π^+ and μ^+ .

The entire range stack is instrumented with transient digitizers (TD)[43] to measure the $\pi^+ \to \mu^+ \to e^+$ decay chain. Four sectors are multiplexed together into one TD channel. They operate at 500 MHz with up to 10 μsec of data from 8-bit flash ADC's. A custom macro-cell chip provides zero suppression and a custom ASIC provides a decision on whether the particle is a π^+ or μ^+ in 10–15 μsec for the Level 1.1 trigger. The Level 1.1 π^+ decision is based on finding a detached second pulse within 180 ns or a single pulse with a large area-to-height ratio, consistent with a π^+ to μ^+ decay, in the stopping counter. TD data from both ends of 4 adjacent RS layers is shown in Fig 7. The pion, entering from layer 11, is seen to stop in layer 12, decay to

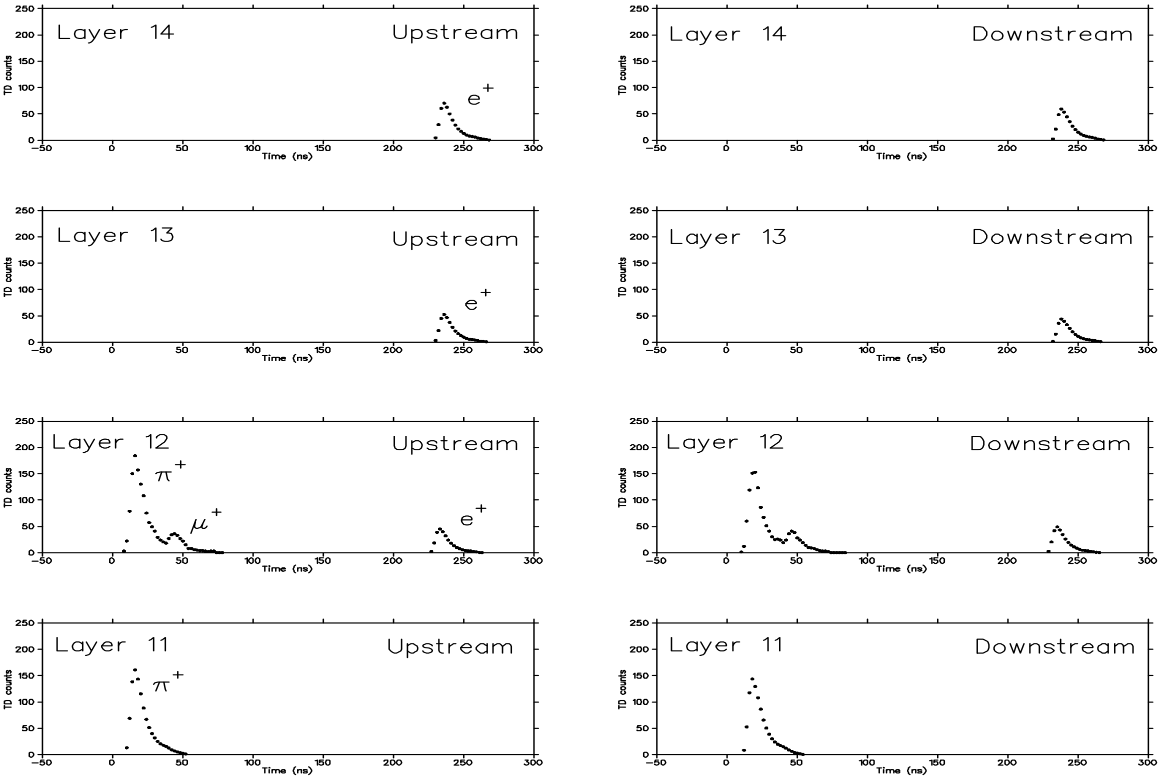

Figure 7: TD data from four adjacent RS layers. A π^+ enters from below (layer 11), stops in layer 12, decays to a μ^+ 20 ns later, and finally decays to an e^+ 190 ns later.

a muon which then decays to an electron. In the offline analysis, the pulse from the stopping counter is fit for both a 1-pulse and 2-pulse hypothesis. Muons are rejected by requiring good 2-pulse fits in both ends, energy consistent with a $\pi^+ \to \mu^+ \nu_\mu$ decay, agreement of the times of the π^+ and μ^+ from both ends and a good e^+ found in the region near the stopping counter.

The E787 photon veto system consists of: a barrel veto (BV), two endcaps (EC), two collar counters (CO) located outside of the EC's, a micro-collar (CM) located further downstream of the downstream CO and an active degrader upstream of the target. The BV consists of 48 sectors and 4 layers of Pb-scintillator sandwich, read out by a PMT on each end. The BV surrounds the RS, 2π in azimuth and 1.9 m axially. The total thickness of the BV is 14.3 $X_\circ$. The E949 photon veto system, will have several additional detectors, principally a barrel veto liner (BVL), between the RS and present BV.

The BVL system, shown in Fig. 8, consists of 48 modules of Pb-scintillator ar-

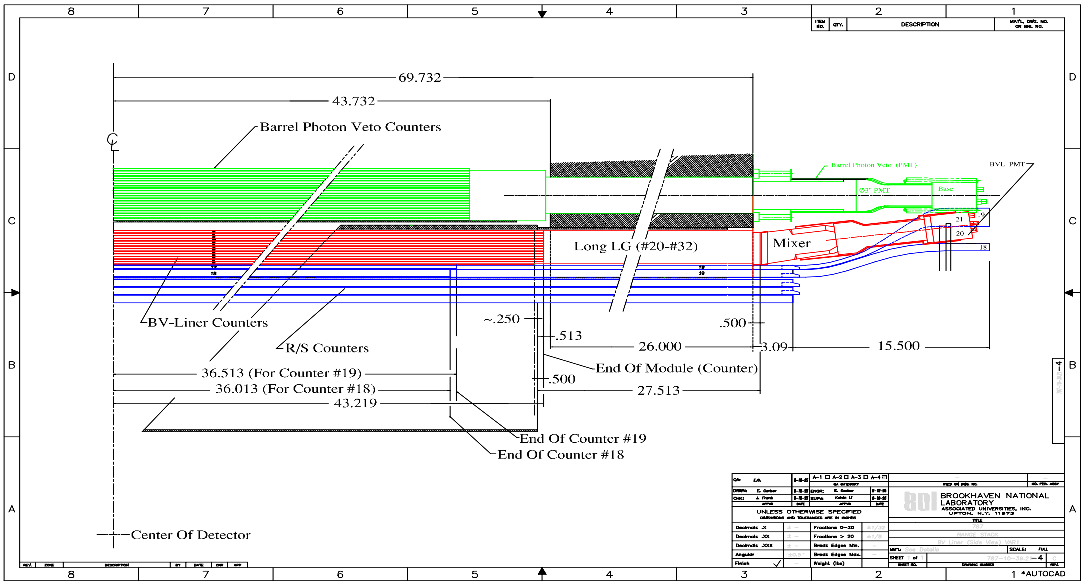

Figure 8: Side view of one half of one module of the barrel veto liner. The BVL (red) lies radially between the outer layers of the RS (blue) and the inner layer of the BV (green).

ranged in 48 azimuthal sectors. Each 2.20 m long module has 13 layers of 5 mm thick Bicron BC408 scintillator, and 12 layers of 1 mm thick lead, for a total of 2.3 $X_\circ$. This system is ready for installation. A few of the completed BVL modules were tested in the AGS test beam, where their performance characteristics were verified. The measured attenuation lengths, 160–180 cm, compare favorably with the existing barrel veto, 80–150 cm. The BVL is a factor of 3 brighter than the existing BV system and provides >30 photoelectrons/MeV/side. It adds critical live material in a thin region of the E787 detector near 45°, and thus is expected to significantly improve the photon vetoing power of the entire detector. It will be especially effective in reducing the $K_{\pi 2}$ background in the region below the $K_{\pi 2}$ peak.

The endcaps[44–46] consist of 143 crystals of pure-CsI, arranged in four concentric rings. The crystals in the inner rings are read out by 2" PMT's and the others are read out by 3" PMT's[45], all in the 1 T magnetic field. The crystals are fully active and have excellent light output. The timing resolution, ~600 ps, is critical in the endcap, which is subject to the highest rates in the detector.

The CO and CM systems are both Pb-scintillator and provide coverage of photons at small angles. In the beam direction, the E787 experiment mounted a 10 cm lead glass (PbG) photon detector on the downstream end of the Beryllium-oxide (BeO) degrader. The E787 photon veto thickness is only 4–7 $X_\circ$ along the beam line in the forward and backward directions. For photons in the relevant energy range this implies a pass-through inefficiency as high as a few percent. For reasons discussed below, it is important to reduce this inefficiency in order to suppress the $K_{\pi 2}$ background below the peak. This can be accomplished by a small supplemental veto counter downstream of the fiber target, and on the upstream end by making more of the K^+ degrader 'live' with the addition of new detectors. In addition to the photon veto detectors listed above, the entire detector is used to veto energy that is not associated with the charged track. A plot of the thickness of the photon veto with and without the BVL is shown in Fig 9.

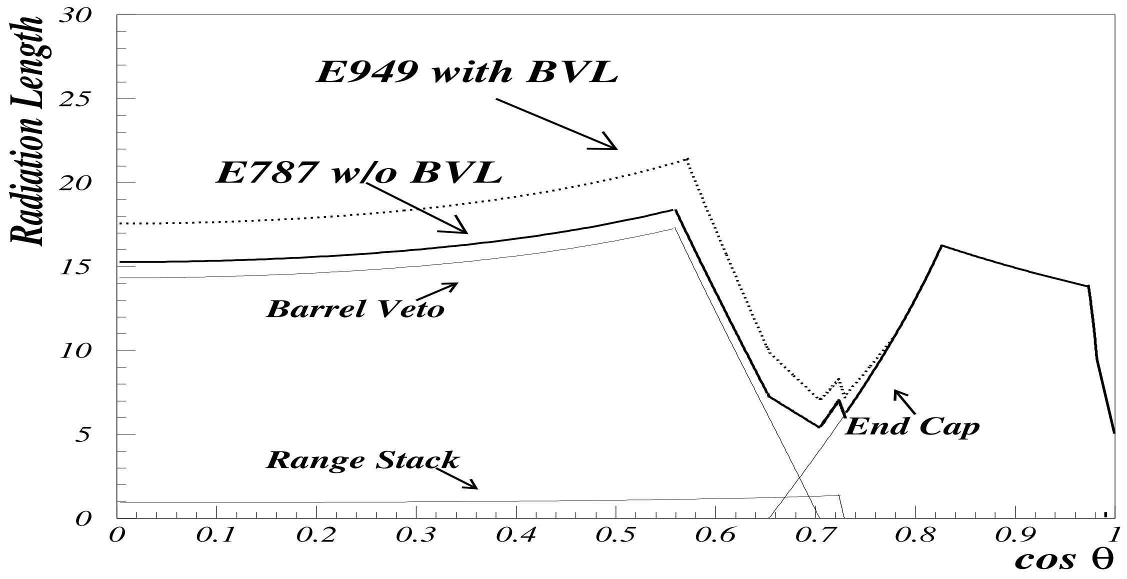

Figure 9: Thickness of E949 with the BVL, compared to the E787. The thickness is shown in radiation lengths versus the polar angle from the z-axis, assuming a point source at the center of the detector.

Approximately 1,000 channels of transient digitizers based on GaAs CCD's[47] have been instrumented on the TT, EC, BV and beam systems. These 500 MHz 8-bit CCD's have ranges of 256 or 512 ns. They have improved the timing resolution and the double pulse resolution for these systems.

The trigger consists of 2 levels. The first, Level 0, requires a kaon stopping in the target, a decay at least 1.5 ns later, no photons in the BV, EC or RS, a range longer than the $K^+ \to \pi^+\pi^+\pi^-$ and shorter than the $K_{\mu 2}$. This part of Level 0, as measured by E787 provides a rejection of $\sim$800. The E949 Level 0 trigger will be pipelined, thereby removing about 30% of the deadtime compared to E787. In addition, detailed track and photon pattern finding will be available for additional trigger rejection. The second level trigger, Level 1, has two components: Level 1.1, as described above requires a $\pi^+ \to \mu^+$ decay in the stopping counter, Level 1.2, requires that no energy is deposited in non-stopping counters in the stopping TD channel and no energy is deposited in the counter radially outward from the stopping counter. The combined Level 1 rejection is $\sim$20.

The DAQ[48–52] is Fastbus based, with front-end readout into Slac Scanner Processors (SSP). The data are transferred via the Cable Segment to VME processors (200 MHz Power PC's). The data are transferred between spills from the VME processors to an 8-CPU SGI Origin 2000. The E787 data transfer capability with an older computer was demonstrated to be >50 Mbytes per spill. It is calculated that the E787 system could maintain 80 Mbytes/spill. The deadtime, which is dominated by the readout of the front-end modules into the SSP's, was $\sim$17% per MHz of stopped kaons (KB) (down from 28% in 1995). The DAQ system has been substantially upgraded already. The addition of a fourth Cable Segment and VME processor are needed for running at the proposed throughput.

3.2 Sensitivity Improvements

The significant features that allow E949 to reach higher levels of sensitivity are listed below. These items are listed as independent gains, whereas, in fact, they have been included, along with the correlations between them in a calculation of the optimum running conditions as described in the next section. Some of these gains are dependent on the rate of incident kaons or on the rate of stopped kaons.

1. Improved fraction of incident K^+ that come to rest in the center of the apparatus. At 790 MeV/c, 19% of the K^+ 's incident on the detector can be brought to rest in the kaon stopping target. Most of the remainder interact or scatter in the degrader just upstream of the stopping target, and cause acceptance losses due to accidental hits in the detector. By removing some of the degrader and transporting a lower momentum K^+ beam, the fraction of the incident kaons stopping in the target increases. The increase in sensitivity is proportional to the increase in the stopping fraction. The increase in stopping fraction has been measured during the 1995–98 runs. E949 will run at $\sim$730 MeV/c, with a stopping fraction of 26%, which will provide an improvement factor of 38% with respect to the 1995 running conditions.

2. Increased spill length. During 1995 the average duty factor was 41%. By increasing the spill length to 4.1 sec (64% Duty Factor) the sensitivity per hour increases by 56%.

3. Increased efficiency already obtained. During the 1997 run, an additional factor of two in trigger rejection was achieved, with improved efficiency, as a result of the addition of the Level 1.2 trigger. The trigger efficiency (Level 1.1) relative to 1995 has been increased by 27% and the experimental deadtime has been reduced from 28% to 17% per MHz of stopped kaons. At the same time, the time range of the TD's to look for the Michel electron from $\mu^+ \to e^+\nu_e\overline{\nu_\mu}$ decay has been extended, with a $\geq$5% acceptance improvement. These factors yield 54% more sensitivity.

4. Additional efficiency improvements. The deadtime will be reduced by at least an additional 5% per KB(MHz). Replacement of the trigger counter counters to provide more light output will increase the trigger efficiency by 8%. Upgrades to the electronics forming the online BV and RS veto signals should gain an additional 4%. Based on the analysis of the 1995–97 data set and the increased statistics on the background samples expected in E949, an increase in acceptance of 30% is likely with a background level of $\sim$10% of the SM. Additional trigger and DAQ efficiency improvements should provide an additional 20% gain. The addition of RS TDC's, extending the time for accepted $\mu^+ \to e^+$ decays to 20μsec will increase acceptance by 5%. Improvements to the offline production software will yield a $\sim$10% increase in acceptance. These incremental improvements should combine to provide a factor of 2.1 increase in the sensitivity.

5. Reduced rate-sensitive acceptance loss from online photon veto, deadtime and offline analysis selection criteria. In addition to the online photon veto and deadtime improvements listed above, improvements to the rate-dependence of the offline analysis are expected. In offline analysis, the rate-dependent selection criteria, namely the photon veto, TD and beam counter cuts will be loosened and compensated for by the less rate-dependent kinematic and target pattern recognition cuts. These effects are presently under study and may yield up to a factor of 2 gain in sensitivity.

   Secondly, additional acceptance from below the $K_{\pi 2}$ may also be achievable. The additional radiation length provided by the BVL will provide a factor of two improvement in the photon veto capability as indicated previously. Improved photon detectors in the beam direction, where the photon veto is presently weak will provide a significant increase in background rejection capability. This is because for the $K_{\pi 2}$ event, in which the π^+ is initially emitted along the beam axis but scattered into the accepted solid angle, the photons from the π° decay tend to be emitted along the beam axis. Once this correlation has been suppressed, the $K_{\pi 2}$ background estimation will be more reliable and the acceptance may be increased by up to a factor of two.

   While the expected improvement from these last two items is a factor of four, they are conservatively counted as a combined factor of two.

The net increase in sensitivity per year (relative to the published 1995 result) from these improvements (items 1– 5 above) is $\sim$14 and is summarized in Table 1. In order to achieve this increase in sensitivity for E949 the number of protons on target will be increased to 65 Tp/spill. All of the requirements from the AGS for this experiment are well within the expected AGS operating parameters for the year 2000. The AGS intensity has increased significantly, to more than 70 Tp, and with the 'barrier bucket' should reach >100 Tp[53]. The AGS duty factor has simultaneously increased, from 37% in early 1995 to 49% in 1998. It is expected that there should be no problems in increasing this to 65% or more[54]. The cooling requirements for the production target for this experiment (with 16 Tp/sec) are less than has already been demonstrated for the E787 target[55].

Upgrade	Improvement factor
Lower momentum	1.38
Higher duty factor	1.56
E787 improvements	1.54
Additional efficiency improvements	2.1
Phase space below $K^+ \to \pi^+\pi^\circ$	(2)
Optimization at higher rate	(2)
Total	14

Table 1: Sensitivity improvement factors for E949, compared to the running conditions of the published E787 result.

3.3 Running Conditions and Expected Sensitivity

A reliable calculation of the sensitivity of E949 in the region above the $K_{\pi2}$ is possible due to the large amounts of data available from E787. Measurements of the K^+ production and the fraction of kaons that stop in the scintillating fiber target have been made as a function of K^+ momentum. The deadtime of the E787 trigger and DAQ, the acceptance of the offline analysis cuts and online trigger have been measured as a function of rate. From these data, the sensitivity of E949, as a function of spill length, kaon momentum, and protons on target has been studied. Contour plots of the sensitivity are shown for E787's 1995 conditions (13 Tp) and for E949 (65 Tp) in Fig. 10a–b.[2] The maximum sensitivity for the 1995 conditions is 1.46×10^6/hr

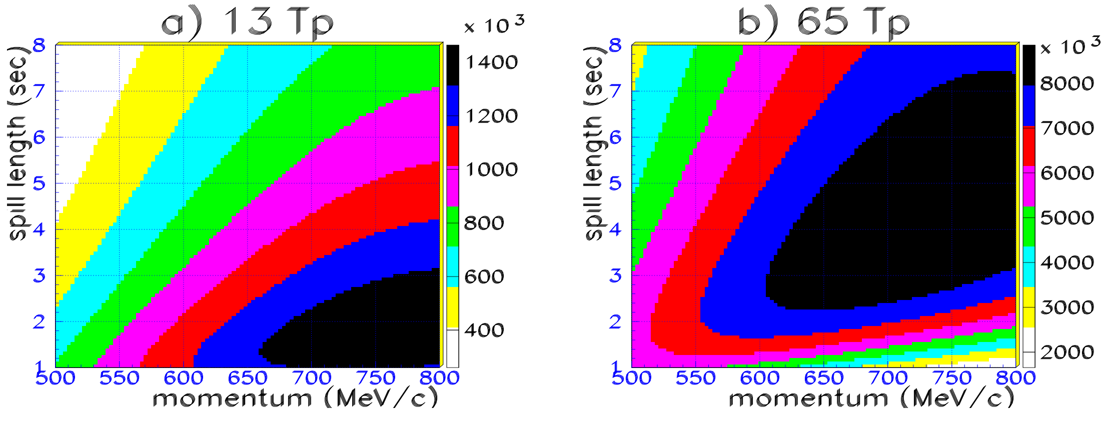

Figure 10: Contours of constant sensitivity/hr for E787 as run in 1995 (13 Tp) and for E949 at 65 Tp (for the region above the $K_{\pi2}$).

at 780 MeV/c and a 1.7 sec spill (see Fig. 10a). These conditions are, in fact, quite close to the actual E787 running conditions in 1995.

The maximum sensitivity at 65 Tp (see Fig. 10b), which is the proposed running condition for this experiment, is 8.9×10^6/hr at 730 MeV/c and 4.1 sec spill every 6.4 sec, which is 6 times larger than the 1995 sensitivity and validates the estimates from

[2]Neither calculation includes AGS or experimental running inefficiencies.

year	KB_L (10^{12})	$\lvert\vec{p_K}\rvert$	DF (%)	sf (%)	$(\text{S.E.S.})^{-1}$ (10^{10})	bck events
1995	1.49	790	41	18.7	0.24	0.08
1995–98	6.2	670–790	47	24	1.2	0.16
2001–02	18	730	64	26	5.3	0.7

Table 2: Comparative Sensitivities. The number of stopped kaons collected on tape (KB_L) has been measured for 1995–98 and is estimated for 2001–2. The reduction of the incident kaon momentum (p_K) has led to an increase the fraction of stopping kaons (sf). The AGS duty factor (DF) has increased over the same time period. The expected sensitivity (S.E.S.$^{-1}$) and number of background events (bck) for the region above the $K_{\pi 2}$ peak are scaled from the published 1995 result, including online trigger and offline acceptance improvements.

the previous section for the region above the $K_{\pi 2}$ peak. If the AGS is able to deliver 100 Tp to the C-target, the experiment can be re-optimized for higher intensity. For example, at 100 Tp the optimum running conditions are 710 MeV/c with a 5.3 sec spill. The sensitivity gain in this case is 13%. A plot showing the optimum sensitivity as a function of protons on target is shown in Figure 11.[3]

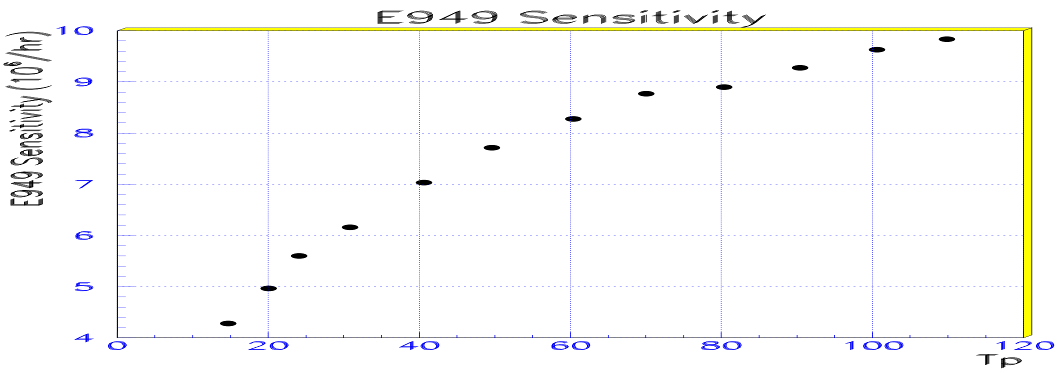

Figure 11: The sensitivity of E949 per hour of running, as a function of protons on the C-target.

After the proposed running time of 6,000 hours ($\sim$2 years), the expected sensitivity will be $(5.3 \times 10^{10})^{-1} = 1.9 \times 10^{-11}$. Combined with the E787 result, the sensitivity should reach 1.5×10^{-11} with 0.8 expected background events. With the added acceptance from the region below the $K^+ \to \pi^+ \pi^\circ$, the sensitivity should reach 8.4×10^{-12}. Therefore the expected number of SM events is 7–12, if the branching ratio is the central SM value of 10^{-10}.

The sensitivity of this experiment is compared to the existing E787 data, including the published 1995 result, in Table 2.

A plot showing progress in sensitivity to $K^+ \to \pi^+ \nu \overline{\nu}$ is shown in Fig 12. Included

[3]It is assumed that to reach $\geq$80 Tp the inter-spill period is increased by 200 msec.

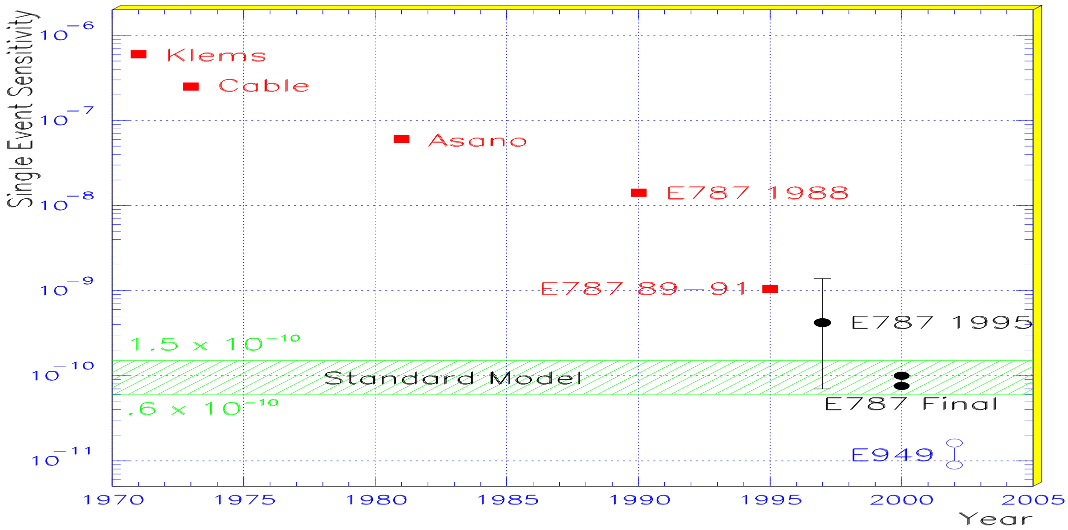

Figure 12: History of progress in the search for $K^+ \to \pi^+ \nu \overline{\nu}$. The solid squares represent single event sensitivities for experiments that set limits on the branching ratio. The solid circles represent the measured and expected sensitivities for the E787 observation of this decay. The open circles represent the expected sensitivity for E949, combined with previous running.

are experiments that set 90% CL limits (earlier E787 results[56–59] and previous experiments[60–62]), as well as the single event sensitivities for E787 and this proposal.

3.4 Background Estimates

Reliable estimation of backgrounds is one of the most important aspects of the measurement of $K^+ \to \pi^+ \nu \overline{\nu}$ at the 10^{-10} level. An identified K^+ is required to stop in the target followed, after a delay of at least 2 ns, by a single charged-particle track that is unaccompanied by any other decay product or beam particle. This particle must be identified as a π^+ with P, R and E between the $K_{\pi 2}$ and $K_{\mu 2}$ peaks for the high energy phase space region or well below the $K_{\pi 2}$ peak for the lower energy region. To elude rejection, $K_{\mu 2}$ and $K_{\pi 2}$ events have to be reconstructed incorrectly in P, R and E. In addition, any event with a muon has to have its track misidentified as a pion — the most effective weapon here is the measurement of the $\pi^+ \to \mu^+ \to e^+$ decay sequence which provides a suppression factor 10^{-5}. Events with photons, such as $K_{\pi 2}$ decays, are efficiently eliminated by exploiting the full calorimeter coverage. The inefficiency for detecting events with π° 's was 10^{-6} in E787 for a photon energy threshold of $\sim$1 MeV. A significant improvement in π° detection efficiency is expected in E949 as indicated earlier. A scattered beam pion can survive the analysis only if misidentified as a K^+ and if the track is mismeasured as delayed, or if the track is missed entirely by the beam counters after a valid K^+ stopped in the target. Kaon charge exchange

(CEX) background events can survive only if the K_L° is produced at low enough energy to remain in the target for at least 2 ns, and if there is no visible gap between the beam track and the observed π^+ track, and if the additional charged lepton went unobserved.

In developing the required rejection criteria (cuts), the redundant and independent constraints available on each source of background are used to establish two independent sets of cuts. One set of cuts is relaxed or inverted to enhance the background (by up to three orders of magnitude) so that the other group can be evaluated to determine its power for rejection. For example, $K_{\mu 2}$ (including $K^+ \to \mu^+ \nu_\mu \gamma$) are to be studied by separately measuring the rejections of the TD particle identification and kinematic cuts. The background from $K_{\pi 2}$ is evaluated by separately measuring the rejections of the photon detection system and kinematic cuts. The background from beam pion scattering is evaluated by separately measuring the rejections of the beam counter and timing cuts. K^+ charge exchange in the target was measured in E787. This data combined with Monte Carlo simulation of semi-leptonic K_L° decays, allows the CEX background to be determined. Small correlations in the separate groups of cuts are investigated for each background source and corrected.

In the E787 1995 data set, the total background level anticipated in the signal region with the final analysis cuts was $b = 0.08 \pm 0.03$ background events (see Table 3). Further confidence in the background estimates and in the measurements of

Background	E787 (1995)	E949
$K_{\pi 2}$	0.03 ± 0.02	0.31
$K_{\mu 2}$	0.02 ± 0.02	0.32
Single beam	0.012 ± 0.009	0.07
Double beam	0.007 ± 0.007	0.04
CEX	0.01 ± 0.01	0.08
Total	0.08 ± 0.03	0.8

Table 3: Background levels (events) measured for the E787 1995 data set, which had a S.E.S. $= 4.2 \times 10^{-10}$ and for E949 (1995–02), with an expected S.E.S. $= 1.5 \times 10^{-11}$. Both cases are for the region above the $K_{\pi 2}$ peak.

the background distributions near the signal region was provided by extending the method described above to estimate the number of events expected to appear when the cuts were relaxed in predetermined ways so as to allow orders of magnitude higher levels of all background types. Confronting these estimates with measurements from the full $K^+ \to \pi^+ \nu \overline{\nu}$ data, where the two sets of cuts for each background type were relaxed simultaneously, tested the independence of the two sets of cuts. At the level of $20 \times b$, two events were observed where 1.6 ± 0.6 were expected, and at $150 \times b$, 15 events were found where 12 ± 5 were expected. Under detailed examination, the events admitted by the relaxed cuts were consistent with being due to the known background sources. Within the final signal region, additional background rejection was available. Therefore, prior to looking in the signal region, several sets of increasingly tighter criteria were established which were designed to be used only to interpret any events that fell into the signal region. Table 3 summarizes the background levels measured in 1995 and projected to E949.

3.5 Sensitivity to $|V_{td}|$

Based on the estimated 10% systematic uncertainty, $|V_{td}|$ would be determined to 30% if the central value of the SM prediction is measured[63] (assuming a 5% uncertainty on $|V_{cb}|$). With the added sensitivity from the region below the $K^+ \to \pi^+\pi^\circ$, the uncertainty on $|V_{td}|$ would be 20%. This precision is comparable to that obtained from measurements of B_d°—$\overline{B_d^\circ}$ mixing. In the latter case the limit on the precision is less reliable since it comes from the theoretical difficulty in calculating the hadronic matrix element[64]. This proposed experiment is free of such difficulties. Eventually measurements of $|V_{td}|$ from the B sector with better theoretical uncertainty are expected (e.g. from measuring B_s°—$\overline{B_s^\circ}$ as well as B_d°—$\overline{B_d^\circ}$ mixing) and the comparison with the $K^+ \to \pi^+\nu\overline{\nu}$ result will become very interesting from the point of view of probing beyond the Standard Model[15,22–24] using only theoretically unambiguous quantities.

4 Cost and Schedule

Upgrades will be needed for the LESB3 beamline, including spare upstream magnets with radiation-hard coils, a new target station, new beam instrumentation, upgrades to reduce radiation levels, and upgrades and maintenance for the electrostatic separators.

Upgrades to the detector, to increase background rejection and efficiency, include the photon veto system, the beam instrumentation, the DAQ and the trigger. The primary tool for reducing background in the region below the $K_{\pi 2}$ is the enhanced photon veto system. The BVL has been built and assembled and will be installed into the detector in FY99. This installation will require 6–9 months. Additional photon veto rejection will be obtained with replacement of the current BeO/PbG degrader, and small supplementary veto systems near the beam. Upgrades to the beam instrumentation include improved position resolution in the B4 counter from the use of overlapping triangular scintillators and the aforementioned more fully active degrader. Additional background rejection power will be gained with the addition of a z-measurement system on the target, from replacement of broken RSSC's, repairs of RS light guides and replacements of some PMTs. The DAQ system will require the addition of a fourth Cable Segment. The DAQ deadtime will be reduced by a reduction in the amount of TD data, with the addition of TDC's on the RS and a shortening of the TD gate width. Additional efficiency improvements through upgrades of the trigger electronics, particularly the online RS and BV vetos, are planned. Further trigger efficiency improvements will be achieved via improvement of the p.e. yield from the T-counters.

With these improvements the E949 experiment will reach a sensitivity of more than five times greater than the entire E787 experiment in only 6,000 hours of running. Given sufficient resources, E949 will be ready to start data collection in the fall of 2000. The upgrades have been chosen to facilitate an early start and rapid conclusion of this experiment.

The total capital cost for DOE is $1.84 M, which is leveraged by a $1.8 M in-kind contribution from Canadian, Japanese and Russian collaborators. The cost estimate is derived from the Work Breakdown Structure (WBS) described in Section 4.1.

4.1 Work Breakdown Structure

The E949 project has been costed in FY00 dollars ($k). The capital request to DOE is for $1.84 M. A summary of the project cost is provided in Figure 13. The

Cost Estimate

(FY00 $k)

WBS #	Title	Material			Labor				Total	Contingency	Total
		Direct	Indirect	Total	FTE	Direct	Indirect	Total	no cont.		
		($k)	($k)	($k)	(man-month)	($k)	($k)	($k)	($k)	($k)	($k)
1	E949 Total	1374.18	310.68	1684.86	191.55	1329.41	751.29	2080.70	3765.56	795.17	4560.74
1.1	AGS	540.50	134.73	675.23	41.75	340.95	203.70	544.65	1219.88	182.98	1402.86
1.1.1	Primary Beam	6.00	2.22	8.22	9.56	81.04	42.85	123.88	132.10	19.82	151.92
1.1.2	Secondary Beam	497.50	115.53	613.03	27.77	224.19	137.67	361.86	974.89	146.23	1121.12
1.1.3	Instrumentation	37.00	16.99	53.99	4.41	35.72	23.18	58.90	112.89	16.93	129.82
1.2	E949 Detector	833.68	175.95	1009.62	149.80	988.46	547.59	1536.06	2545.68	612.19	3157.87
1.2.1	Detector Systems	289.75	67.12	356.87	85.80	583.85	322.02	905.86	1262.74	330.86	1593.60
1.2.2	Electronics	428.98	88.30	517.29	55.00	351.28	195.84	547.11	1064.40	233.49	1297.89
1.2.3	Monitor	114.94	20.53	135.47	9.00	53.34	29.74	83.08	218.54	47.84	266.38

Figure 13: Summary of the E949 WBS. This is the total capital cost for the experiment, including full overhead charges and the cost to build components that will be supplied by foreign collaborators.

proposed funding plan for the project is shown in Figure 14. Significant in-kind contributions already confirmed from Canada, Japan, and Russia will leverage the DOE contribution by a large factor.

Proposed Funding Plan

(FY00 $k)

Canadian Contribution (in-kind)	1078.01
Japanese Contribution (in-kind)	564.93
Russian Contribution (in-kind)	213.12
BNL Physics Department HEP Base Program	867.42
BNL HEP Equipment	1837.26
Total	4560.74

Figure 14: Proposed funding plan for E949.

A contribution from the base BNL physics department program comparable to the level for E787 (six technicians per year) is assumed. The contributions from international collaborators are costed in terms of BNL burdens and labor charges.

The capital contribution from the reuse of major portions of the E787 detector is not included in the cost estimate.

The large amount of labor costs associated with the E949 project arise from two factors. One is the large effort involved to open and then re-close the detector. The other is the fact that most of the construction of one major system, the BVL, is already completed and most of what remains is the installation.

The schedule is provided in Figure 15. With minimal funding in FY99 and a substantial increase in FY00 this experiment will be ready for collecting data in FY01.

Construction Plan by Year

(FY00 $k)

Total Cost	FY99	FY00	FY01
1837.26	117.00	1300.00	420.26

Figure 15: Construction plan for the E949 project.

A flow chart, showing the major effort for the E949 project is provided in Figure 16.

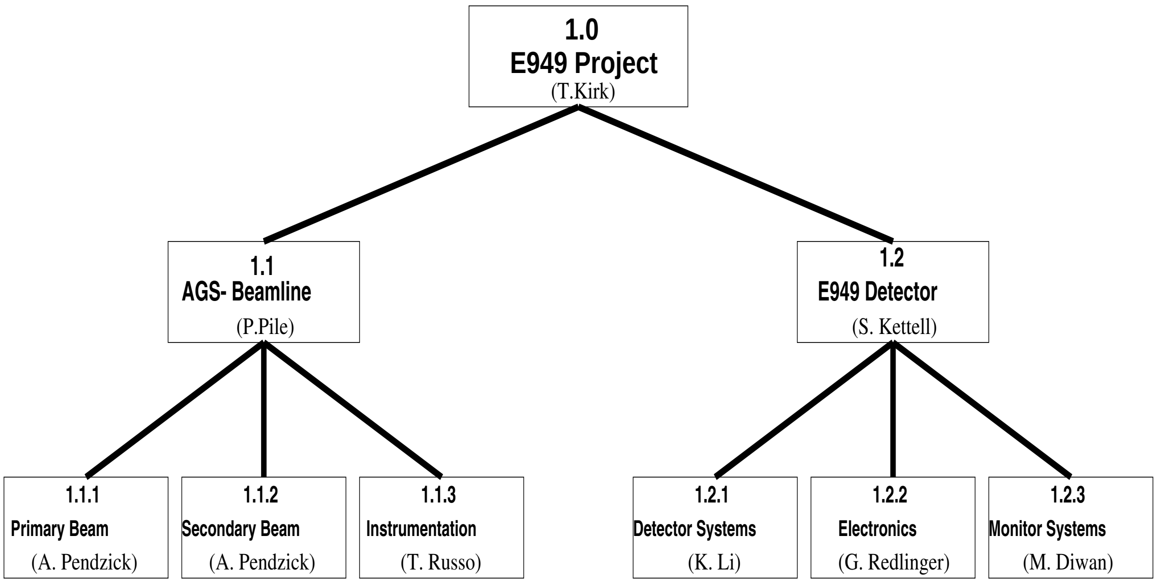

Figure 16: Flow Chart of the E949 WBS.

The cost basis of estimate relies on recent as-built costs for

- AGS secondary beam (1.1.2)

- AGS instrumentation (1.1.3)
- Range Stack (1.2.1.7)
- DAQ (1.2.2.2.4–8)

plus upgraded designs for improved versions of previously built items, such as,

- Detector systems (1.2.1.1–6,8)
- AGS primary beam (1.1.1)
- Trigger (1.2.2.1.2–4)
- Cable segment (1.2.2.2.3)
- RS gain monitor (1.2.3.3)

and as-quoted purchases for

- DAQ (1.2.2.2.1–2)
- Trigger (1.2.2.1.1,6)
- Monitor (1.2.3.1–2,4) .

Recent estimates for this type of project are consistent with a contingency of 30% for the labor on the types of work involved. A contingency of 5% on catalog purchases obtains from the typical quoted validity term of 30 days. The contingency of 25% on subcomponent procurement derives from recent experience with similar projects. The contingency of 15% on all AGS projects is based on previous experience with similar projects. The costs are shown in detail in Figures 17–22.

AGS Primary Beam Costs

WBS #	Title	Material			Labor				Total	Contingency	Total
		Direct	Indirect	Total	FTE	Direct	Indirect	Total	no cont.		
		($k)	($k)	($k)	(man-month)	($k)	($k)	($k)	($k)	($k)	($k)
1.1.1	Primary Beam	6.00	2.22	8.22	9.56	81.04	42.85	123.88	132.10	19.82	151.92
1.1.1.1	Beam Dump	0.00	0.00	0.00	9.20	78.15	40.87	119.02	119.02	17.85	136.87
	Includes removal of C1D2, C3C1, C1Q3,C1Q4										
	C1D3,C1D4 and C3D4 and installation of a primary beam dump										
1.1.1.2	C-target	6.00	2.22	8.22	0.37	2.89	1.98	4.87	13.09	1.96	15.05
	Two New C-Targets	6.00	2.22	8.22						1.23	9.45

Figure 17: E949 WBS 1.1.1: AGS Primary Beam.

AGS Secondary Beam Costs												
WBS #	Title	Material			Labor				Total	Contingency	Total
		Direct	Indirect	Total	FTE	Direct	Indirect	Total	no cont.		
		($k)	($k)	($k)	(man-month)	($k)	($k)	($k)	($k)	($k)	($k)
1.1.2	Secondary Beam	497.50	115.53	613.03	27.77	224.19	137.67	361.86	974.89	146.23	1121.12
1.1.2.1	Replace Q1-2	0.00	0.00	0.00	3.13	24.84	15.24	40.08	40.08	6.01	46.10
1.1.2.2	New Q1-2	145.50	35.67	181.17	8.51	68.38	45.03	113.41	294.58	44.19	338.77
	Q01(N8Q24)										
	Steel Core	20.00	4.18	24.18						3.63	27.81
	Radiation Hard Coils	55.00	11.50	66.50						9.98	76.48
	Misc. Hardware	10.50	4.82	15.32						2.30	17.62
	Q02(N8Q12)	0.00	0.00	0.00							
	Steel Core	12.00	2.51	14.51						2.18	16.69
	Radiation Hard Coils	37.50	7.84	45.34						6.80	52.14
	Misc. Hardware	10.50	4.82	15.32						2.30	17.62
1.1.2.3	New D1	347.00	77.56	424.56	4.69	37.85	24.14	61.99	486.55	72.98	559.53
	Steel Core	97.00	20.28	117.28						17.59	134.88
	Radiation Hard Coils	205.00	42.87	247.87						37.18	285.05
	Vacuum Box	25.00	5.23	30.23						4.53	34.76
	Misc Hardware	20.00	9.18	29.18						4.38	33.56
1.1.2.4	Reroute Q1-2 water	5.00	2.30	7.30	6.67	54.37	30.27	84.64	91.94	13.79	105.73
1.1.2.5	Separator	0.00	0.00	0.00	4.78	38.75	22.99	61.74	61.74	9.26	71.00

Figure 18: E949 WBS 1.1.2: AGS Secondary Beam.

AGS Instrumentation Costs												
WBS #	Title	Material			Labor				Total	Contingency	Total
		Direct	Indirect	Total	FTE	Direct	Indirect	Total	no cont.		
		($k)	($k)	($k)	(man-month)	($k)	($k)	($k)	($k)	($k)	($k)
1.1.3	Instrumentation	37.00	16.99	53.99	4.41	35.72	23.18	58.90	112.89	16.93	129.82
1.1.3.1	Primary beam	36.00	16.53	52.53	4.18	34.01	22.01	56.02	108.55	16.28	124.83
	Remove CW474 SWIC	0.00	0.00	0.00	0.05					0.00	0.00
	Replace CW475 SWIC	1.00	0.46	1.46	0.23					0.22	1.68
	Replace C-SEC and Table	28.00	12.85	40.85	1.38					6.13	46.98
	Upgrade C-target Temperature monitor	0.00	0.00	0.00	1.15					0.00	0.00
	Replace C-target flag camera	2.00	0.92	2.92	0.69					0.44	3.36
	Replace 90 Degree monitor	5.00	2.30	7.30	0.69					1.09	8.39
1.1.3.2	Secondary beam	1.00	0.46	1.46	0.23	1.71	1.17	2.88	4.34	0.65	4.99
	Replace Rad-Damaged Cable for C2W569 & C2W606										

Figure 19: E949 WBS 1.1.3: AGS Instrumentation.

Costs of Detector Systems

WBS #	Title	Material			Labor				Total	Contingency	Total
		Direct	Indirect	Total	FTE	Direct	Indirect	Total	no cont.		
		($k)	($k)	($k)	(man-month)	($k)	($k)	($k)	($k)	($k)	($k)
1.2.1	**Detector Systems**	**289.75**	**67.12**	**356.87**	**85.80**	**583.85**	**322.02**	**905.86**	**1262.74**	**330.86**	**1593.60**
1.2.1.1	**BVL**	**35.04**	**10.59**	**45.63**	**47.30**	**343.39**	**188.90**	**532.29**	**577.92**	**166.95**	**744.87**
1.2.1.1.1	**Mechanical**	*15.19*	*6.97*	*22.17*	*41.3*	*307.82*	*169.07*	*476.90*	*499.06*	*144.47*	*643.53*
	Remove/Instal				5x8 T+1x8 E	294.12	163.97	458.10	458.10	137.43	595.53
	Jigsaw Pieces/Brackets	3.19	1.46	4.66					4.66	0.23	4.89
	mu-metal shields	11.00	5.05	16.05					16.05	0.80	16.85
	misc.	1.00	0.46	1.46					1.46	0.36	1.82
	Shop Work				1.3	13.70	5.10	18.80	18.80	5.64	24.44
1.2.1.1.2	**Electronics**	*19.85*	*3.62*	*23.47*	*6*	*35.56*	*19.83*	*55.39*	*78.85*	*22.48*	*101.34*
	Remove/Instal				1x6 T	35.56	19.83	55.39	55.39	16.62	72.00
	PMT	14.85	1.32	16.17					16.17	4.04	20.22
	splitter boxes	1.00	0.46	1.46					1.46	0.36	1.82
	cables,connector	4.00	1.84	5.84					5.84	1.46	7.30
1.2.1.2	**Active Degrader**	**61.40**	**11.71**	**73.11**	**5.5**	**37.04**	**19.71**	**56.76**	**129.86**	**24.87**	**154.73**
	Instal				1x2 TE	26.12	14.56	40.68	40.68	12.20	52.88
	PMT	44.55	3.97	48.52					48.52	2.43	50.95
	scintillator	1.50	0.69	2.19					2.19	0.11	2.30
	fiber	1.00	0.46	1.46					1.46	0.07	1.53
	Converter Metal	4.00	1.84	5.84					5.84	1.46	7.30
	Shop Work				0.50	5.00	1.85	6.85	6.85	2.06	8.91
	cabling	6.50	2.98	9.48	1x1 T	5.93	3.30	9.23	18.72	5.14	23.86
	Pulse Shaper	3.85	1.77	5.62					5.62	1.40	7.02
1.2.1.3	**B4 Counter**	**16.46**	**2.76**	**19.22**	**0.00**	**0.00**	**0.00**	**0.00**	**19.22**	**1.84**	**21.06**
	PMT	12.96	1.15	14.11					14.11	0.71	14.82
	scintillator	0.50	0.23	0.73					0.73	0.04	0.77
	cabling	3.00	1.38	4.38					4.38	1.09	5.47
1.2.1.4	**Downstream PV**	**8.49**	**3.90**	**12.39**	**4.00**	**26.12**	**14.56**	**40.68**	**53.07**	**15.30**	**68.37**
	PMT, bases	0.99	0.45	1.44					1.44	0.36	1.81
	cable, electronics	2.00	0.92	2.92					2.92	0.73	3.65
	Lucite, forms	2.50	1.15	3.65					3.65	0.91	4.56
	mount	3.00	1.38	4.38	1x2 TE	26.12	14.56	40.68	45.05	13.30	58.35
1.2.1.5	**T-counter**	**41.00**	**18.82**	**59.82**	**7**	**42.69**	**23.80**	**66.49**	**126.32**	**33.39**	**159.70**
	Removal/Instal	28.80	13.22	42.02	1x1 E	7.13	3.98	11.11	53.13	13.84	66.97
	scintillator	3.60	1.65	5.25					5.25	0.26	5.52
	1mm fiber	1.60	0.73	2.33					2.33	0.12	2.45
	adaptors	3.00	1.38	4.38					4.38	1.09	5.47
	rhoacell	1.00	0.46	1.46					1.46	0.36	1.82
	misc.	1.00	0.46	1.46					1.46	0.36	1.82
	Assembly	2.00	0.92	2.92	3x2 T	35.56	19.83	55.39	58.30	17.35	75.65
1.2.1.6	**RSSC**	**10.20**	**4.68**	**14.88**	**1**	**5.93**	**3.30**	**9.23**	**24.11**	**6.49**	**30.60**
	Removal/Installation	7.20	3.31	10.51					10.51	2.63	13.13
	Assembly/connectors	3.00	1.38	4.38	2x0.5 T	5.93	3.30	9.23	13.61	3.86	17.47
1.2.1.7	**RS**	**23.75**	**2.86**	**26.61**	**10.75**	**65.22**	**36.36**	**101.58**	**128.18**	**32.39**	**160.57**
	Repair Light Guides	1.00	0.46	1.46	3x2.5 T+1.25 E	53.37	29.75	83.12	84.58	25.30	109.88
	PMTs	21.75	1.94	23.69					23.69	1.18	24.87
	Bases	1.00	0.46	1.46	1x2 T	11.85	6.61	18.46	19.92	5.90	25.82
1.2.1.8	**Target**	**38.41**	**6.90**	**45.31**	**5.25**	**31.42**	**17.51**	**48.93**	**94.24**	**19.69**	**113.93**
	PMTs	29.01	2.58	31.60					31.60	1.58	33.17
	Z Measurement System	7.00	3.21	10.21	2x2 T	23.71	13.22	36.92	47.14	13.63	60.77
	Z Installation	2.40	1.10	3.50	4x0.25T+1x0.25	7.71	4.30	12.01	15.51	4.48	19.99
1.2.1.9	**UTC**	**55.00**	**4.90**	**59.90**	**5**	**32.04**	**17.86**	**49.91**	**109.81**	**29.95**	**139.76**
	Preamps	55.00	4.90	59.90	1x3 T+1x2E	32.04	17.86	49.91	109.81	29.95	139.76

Figure 20: E949 WBS 1.2.1: Detector Systems.

Electronics Costs (Trigger/DAQ)											
WBS #	Title	Material			Labor				Total	Contingency	Total
		Direct	Indirect	Total	FTE	Direct	Indirect	Total	no cont.		
		($k)	($k)	($k)	(man-month)	($k)	($k)	($k)	($k)	($k)	($k)
1.2.2	**Electronics**	**428.98**	**88.30**	**517.29**	**55.00**	**351.28**	**195.84**	**547.11**	**1064.40**	**233.49**	**1297.89**
1.2.2.1	**Trigger**	**67.90**	**12.67**	**80.57**	**25.00**	**157.81**	**87.98**	**245.79**	**326.36**	**93.88**	**420.24**
1.2.2.1.1	**BV Meantimer**	1.90	0.87	2.77	0.5	2.96	1.65	4.62	7.39	2.08	**9.47**
	Cabling	1.90	0.87	2.77	1x0.5 T	2.96	1.65	4.62	7.39	2.08	9.47
1.2.2.1.2	**Pipeline L0**	14.00	6.43	20.43	18	113.91	63.51	177.42	197.85	58.33	**256.18**
	RC Layout				1x3 E	21.40	11.93	33.32	33.32	10.00	43.32
	RC Construction	2.00	0.92	2.92	1x6 T	35.56	19.83	55.39	58.30	17.35	75.65
	RC FPGA	7.00	3.21	10.21					10.21	2.55	12.77
	RC components	1.00	0.46	1.46					1.46	0.36	1.82
	TT Layout				1x3 E	21.40	11.93	33.32	33.32	10.00	43.32
	TT Construction	2.00	0.92	2.92	1x6 T	35.56	19.83	55.39	58.30	17.35	75.65
	TT components	1.00	0.46	1.46					1.46	0.36	1.82
	Software	1.00	0.46	1.46					1.46	0.36	1.82
1.2.2.1.3	**IC Electronics**	1.00	0.46	1.46	0.25	1.48	0.83	2.31	3.77	1.06	**4.82**
	Splitters	1.00	0.46	1.46	1x0.25 T	1.48	0.83	2.31	3.77	1.06	4.82
1.2.2.1.4	**Cer Electronics**	1.00	0.46	1.46	0.25	1.48	0.83	2.31	3.77	1.06	**4.82**
	Splitters	1.00	0.46	1.46	1x0.25 T	1.48	0.83	2.31	3.77	1.06	4.82
1.2.2.1.5	**Trigger Module**	50.00	4.46	54.46	6	37.97	21.17	59.14	113.59	31.36	**144.95**
	Design/Construction	50.00	4.46	54.46	1x2 E+1x4 T	37.97	21.17	59.14	113.59	31.36	144.95
1.2.2.2	**DAQ**	**361.08**	**75.63**	**436.71**	**30.00**	**193.47**	**107.86**	**301.33**	**738.04**	**139.61**	**877.65**
1.2.2.2.1	**RS TDC**	65.42	6.57	71.99	3.00	17.78	9.91	27.69	99.68	12.49	**112.17**
	TDC	63.42	5.65	69.07					69.07	3.45	72.52
	Cabling	2.00	0.92	2.92	1x3 T	17.78	9.91	27.69	30.61	9.04	39.65
1.2.2.2.2	**Computer**	136.63	14.44	151.07					151.07	7.55	**158.62**
	Origin 2000	88.75	7.91	96.66					96.66	4.83	101.49
	DLT Drive	16.58	1.48	18.06					18.06	0.90	18.96
	DLT Stacker	18.78	1.67	20.45					20.45	1.02	21.47
	Disks	6.33	0.56	6.89					6.89	0.34	7.24
	printer	3.71	1.70	5.41					5.41	0.27	5.68
	Network Switch	2.48	1.12	3.60					3.60	0.18	3.78
1.2.2.2.3	**Cable Segment**	64.04	11.20	75.24	1.00	5.93	3.30	9.23	84.47	10.86	**95.33**
	Hybrids	2.00	0.92	2.92					2.92	0.73	3.65
	4th Segment	12.84	5.89	18.73	1x1 T	5.93	3.30	9.23	27.97	7.45	35.42
	SFI upgrade	49.20	4.38	53.58					53.58	2.68	56.26
1.2.2.2.4	**TD Control Board**	26.00	11.94	37.94	4.00	26.12	14.56	40.68	78.61	21.69	**100.30**
	Construction	20.00	9.18	29.18	1x1 TE	13.06	7.28	20.34	49.52	13.40	62.92
	Assembly/Testing	6.00	2.75	8.75	1x1 TE	13.06	7.28	20.34	29.09	8.29	37.38
1.2.2.2.5	**CCD's**	56.00	25.52	81.52	16.00	102.06	56.90	158.96	240.47	62.85	**303.32**
	construction	35.00	16.07	51.07	1x6 TE	78.35	43.68	122.03	173.10	49.38	222.48
	New Cables	3.00	1.35	4.35	1x2 T	11.85	6.61	18.46	22.81	6.63	29.44
	Cable Modifications	18.00	8.10	26.10	1x2 T	11.85	6.61	18.46	44.56	6.84	51.41
1.2.2.2.6	**System Master**	3.00	1.38	4.38	2.00	14.26	7.95	22.22	26.59	7.76	**34.35**
	Modification	3.00	1.38	4.38	1x2 E	14.26	7.95	22.22	26.59	7.76	34.35
1.2.2.2.7	**Cable Seg Coord**	3.00	1.38	4.38	2.00	14.26	7.95	22.22	26.59	7.76	**34.35**
	Construction	3.00	1.38	4.38	1x2 E	14.26	7.95	22.22	26.59	7.76	34.35
1.2.2.2.8	**IO Boards**	7.00	3.21	10.21	2.00	13.06	7.28	20.34	30.55	8.66	**39.21**
	Design/Construct	7.00	3.21	10.21	1x1 TE	13.06	7.28	20.34	30.55	8.66	39.21

Figure 21: E949 WBS 1.2.2: Electronics.

Detector Monitoring System Costs											
WBS #	Title	Material			Labor				Total	Contingency	Total
		Direct	Indirect	Total	FTE	Direct	Indirect	Total	no cont.		
		($k)	($k)	($k)	(man-month)	($k)	($k)	($k)	($k)	($k)	($k)
1.2.3	Monitor	114.94	20.53	135.47	9.00	53.34	29.74	83.08	218.54	47.84	266.38
1.2.3.1	**Voltage Monitor**	**31.05**	**7.02**	**38.07**	**3**	**17.78**	**9.91**	**27.69**	**65.76**	**11.09**	**76.85**
	PC	2.57	1.18	3.75					3.75	0.19	3.93
	Interface Card	6.09	2.74	8.82					8.82	0.44	9.27
	Scanning ADC	19.40	1.73	21.12					21.12	1.06	22.18
	Cables/Connectors	3.00	1.38	4.38	1x3 T	17.78	9.91	27.69	32.07	9.40	41.47
1.2.3.2	**Time Structure Mon**	**17.60**	**1.57**	**19.16**	**1**	**5.93**	**3.30**	**9.23**	**28.39**	**3.73**	**32.12**
	Waveform Analyzer	17.60	1.57	19.16	1x1 T	5.93	3.30	9.23	28.39	3.73	32.12
1.2.3.3	**RS Gain Monitor**	**65.00**	**11.34**	**76.34**	**5.00**	**29.63**	**16.52**	**46.15**	**122.50**	**32.93**	**155.43**
	Light Source	10.00	4.59	14.59					14.59	3.65	18.24
	Fiber Optics	40.00	3.56	43.56					43.56	10.89	54.46
	mounting hardware	10.00	0.89	10.89	1x5 T	29.63	16.52	46.15	57.05	16.57	73.61
	reference PMT	5.00	2.30	7.30					7.30	1.82	9.12
1.2.3.4	**Copier**	**1.30**	**0.59**	**1.89**					**1.89**	**0.09**	**1.98**

Figure 22: E949 WBS 1.2.3: Monitor Systems.

4.2 WBS Dictionary

A description of each of the items in the WBS follows:

1.0 E949: An experiment to measure the branching ratio B($K^+ \to \pi^+ \nu\overline{\nu}$)

- 1.1 AGS: This includes all costs associated with the AGS delivery of beam to the experiment. It is divided into 3 sub categories: the primary proton beam, the secondary kaon beam, and instrumentation.
  - 1.1.1 Primary proton beam: Install a beam dump for the downstream section of the C-line and build new targets to replace the existing C-target.
    - 1.1.1.1 Beam Dump: Installation of a well-shielded re-entrant beam dump for the primary proton beam, downstream of the C-target to reduce ambient radiation levels with high intensity on the C-target.
    - 1.1.1.2 C-Target: Manufacture two new targets to serve as spares for the existing C-target.

1.1.2 Secondary Beam: Replace the first two quadrupole magnets in the C-4 line (with radiation hard coils), a spare for the first dipole magnet in the C-4 line, upgrades to the separators in the C-4 line, and some radiation protection issues.

1.1.2.1 Replace Q01–2: The coils on these magnets have exceeded their expected lifetime from radiation damage and therefore these magnets should be replaced with the existing spares.

1.1.2.2 Make new Q01–2 magnets to serve as spares. This includes the steel, radiation hard coils and associated hardware.

1.1.2.3 Make a new D01 sector magnet to serve as a spare. This includes the steel, radiation hard coils, the vacuum chamber and associated hardware.

1.1.2.4 Reroute Q01–2 water: Rerouting of the cooling water for the upstream magnets into the local heat exchanger system will reduce radiation levels on the AGS floor.

1.1.2.5 Separator upgrades: Redesign of the separator standoff's will allow for more reliable separator operation.

1.1.3 Instrumentation: Upgrades to or replacement of instrumentation in both the primary proton beam and the secondary beam.

1.1.3.1 Primary beam instrumentation: A SWIC for heavy ion operations will be removed to reduce scattering; the SWIC for the C-target servo will be replaced to allow active feedback of the beam position; the C SEC and table will be replaced due to large efficiency loss from radiation damage; the C-target temperature electronics will be upgraded to allow better monitoring of the C-target temperature; the flag camera will be upgraded and the 90° telescope will be replaced and relocated to improve the reliability of the system.

1.1.3.2 Secondary beam instrumentation: This includes new cables for ionization chambers to replace the existing radiation damaged ones.

1.2 E949 Detector: This includes all costs associated with the E949 detector. Elements downstream of the last quadrupole magnet in the C-4 line(Q10). This category is further subdivided into three sub-categories: detector systems, electronics, and monitoring systems.

1.2.1 Detector Systems: Replacement of or repair of existing detector elements at the downstream end of the C-4 beam line. This category is further broken down into nine components (1.2.1.1–9)

1.2.1.1 Barrel Veto Liner(BVL): Opening the E787 (now E949) detector, removal of the outer layers of the range stack (layers 18-21), installation of the BVL, and closing the E949 detector. The BVL system will provide additional photon veto rejection and allow for exploitation of the region below the $K_{\pi 2}$ peak and allow for operation of the detector at higher kaon fluxes.

- 1.2.1.2 Active Degrader: Construction of a new, active degrader to replace the existing Be0 and PbG degrader, with new electronics, cabling, and installation will provide additional photon veto rejection to exploit the region below the $K_{\pi 2}$ peak.
- 1.2.1.3 B4 Counter: Construction of a new, more finely segmented B4 counter, additional cabling, and installation will reduce background from scattered particles in the beam and will improve pattern recognition in the target and hence the determination of the π^+ kinematics.
- 1.2.1.4 Downstream Photon Veto: Modification of existing, prototype BVL modules to be used for a photon veto system downstream of the target, a mounting system, light guides, PMTs, bases, cables, electronics and installation will provide additional photon veto rejection to exploit the region below the $K_{\pi 2}$ peak.
- 1.2.1.5 T-counter: Removal of the inner layers of the range stack (layers 1-4), purchase of grooved scintillator with wavelength shifting fiber to replace layer 1, support structures for the fibers, and the re-installation of the inner 4 layers of the RS will improve the trigger acceptance.
- 1.2.1.6 Range Stack Straw Chambers: Replacement of broken chambers.
- 1.2.1.7 Range Stack: Purchase of 50 new PMTs to replace poorly performing ones and spares for anticipated future failures, repair of existing bad bases and the production of new ones, and removal of light guides with broken or poorly connected joints and the repair of the joints and re-installation of the light guides will improve the light yield and the energy resolution and $\pi^+ \to \mu^+ \to e^+$ determination.
- 1.2.1.8 Target: Purchase and installation of 40 new PMTs to replace poorly performing ones and the installation of an additional system to provide z-information. These will improve the light yield and energy resolution in the target and improve the pattern recognition in the UTC leading to improved π^+ kinematics.
- 1.2.1.9 Ultra Thin Chamber(UTC): Design of a new preamp for the UTC, purchase of components, and the production, testing and installation of the new preamps (2,000 channels) will improve the z-measurement and the π^+ kinematics.

1.2.2 Electronics: Upgrades to the existing trigger and DAQ systems. This category is further subdivided into two sub-categories: the trigger and the DAQ.

- 1.2.2.1 Trigger: This item contains the cost for upgrading the trigger system; it includes five sub-categories (1.2.2.1.1–5).
  - 1.2.2.1.1 Barrel Veto(BV) Meantimer: Assembly of a system to improve the timing of the BV system, will reduce online accidental veto losses.
  - 1.2.2.1.2 Pipeline L0: Design, production and installation of two types of trigger boards: one a replacement for the existing range cards, the second, a deadtime free version of the trigger transmitter and

trigger boards will improve the trigger rejection and reduce trigger deadtime.

1.2.2.1.3 IC electronics: Production of 8 splitter boxes and some re-cabling will improve the trigger efficiency.

1.2.2.1.4 Cerenkov electronics: Production of 30 splitter boxes and some re-cabling may improve the trigger efficiency and will improve the rejection of backgrounds from accidental K^+ .

1.2.2.1.5 Trigger Module: Design, Construction and assembly of a new trigger module that can be remotely programmed to create up to 32 triggers will allow greater flexibility in the trigger and reduce losses from trigger debugging.

1.2.2.2 DAQ: This item includes the cost of upgrading the data acquisition system. This category includes eight sub-items (1.2.2.2.1–8).

1.2.2.2.1 Range Stack TDC: Purchase and installation of a TDC system, with 9 TDC modules and the associated cabling will reduce the deadtime by allowing for a shorter TD gate.

1.2.2.2.2 Computer: Purchase of a more powerful DAQ computer (Origin 2000), 5 disks, 3 DLT tape drives, and a DLT stacker will improve DAQ throughput and will allow an operating cost savings on the tape media.

1.2.2.2.3 Cable Segment Upgrade: Procurement of spare hybrids, the construction of a fourth cable segment, and the replacement of 5 SSP's in the TD system with SFI's will improve DAQ throughput.

1.2.2.2.4 TD Control Board(TDCB): Production of an addition 30 TDCB's for use as spares. This will reduce experimental down-time.

1.2.2.2.5 CCD's: Construction of an additional 160 CCD channels (10 modules) for readout of the new detector elements will improve beam background and photon veto rejection.

1.2.2.2.6 TD System Master(TDSM): Redesign of the TDSM to speed up the clock, testing, installation and construction of a new board will improve the trigger rejection.

1.2.2.2.7 Cable Segment Coordinator(CSC): Production of a PC board version of the CSC will reduce experimental down-time.

1.2.2.2.8 IO Boards: Layout, production and installation of 6 additional IO boards needed for the Cable Segment upgrade.

1.2.3 Monitor: This item includes new systems for monitoring the status of the experiment.

1.2.3.1 Voltage Monitor: PC and CAMAC based data acquisition system to continuously measure voltages and temperatures of equipment in the experiment; PC, interface board and 250 channels of scanning ADC will improve experimental uptime.

1.2.3.2 Time Structure Monitor: Purchase and installation of a Signal Analyzer to provide real-time data on the time structure of the beam delivered by the AGS. This device will take signal input from AGS and E949 systems and provide fast Fourier transforms to determine frequencies of any structure in the delivered beam. This system will be used to help keep the experimental sensitivity optimized.

1.2.3.3 RS Gain Monitor: Triggerable light source to deliver light to the RS PMT's to allow continuous measurement of PMT gains. This includes the light source, fibers to transmit light to the PMTs, supports and connectors for mounting the fibers, and a system for monitoring the stability of the light source itself. This system will maintain experimental uptime and improve the energy resolution.

1.2.3.4 Copier: Purchase of a copier to facilitate reproduction of the logbooks and other documents.

5 Conclusion

The initial observation of $K^+ \to \pi^+ \nu\overline{\nu}$ at the 10^{-10} level inspires this proposal to explore this important rare process to a level of sensitivity one order of magnitude below the Standard Model prediction with minimal expected backgrounds. Modest upgrades of a proven detector provide the opportunity to reveal non-Standard Model physics or to make a precise, unambiguous measurement of $|V_{td}|$. This measurement bears directly on the question of the Standard Model origin of CP violation. Combined with a measurement of $K^\circ_L \to \pi^\circ \nu\overline{\nu}$, the CKM triangle (parameters $\overline{\rho}$ and $\overline{\eta}$) can be accurately determined, providing crucial and unambiguous information from the precisely calculated K system. This information is independent of and complementary to future measurements in the B system. Input from both systems is necessary to confront the Standard Model and search for new physics.

The large amount of $K^+ \to \pi^+ \nu\overline{\nu}$ data collected by experiment E787 supports a confident projection for the E949 experiment to this extraordinary level of sensitivity, an order of magnitude below the Standard Model prediction for the branching ratio. Important issues, such as deadtime, online and offline accidental veto losses, trigger and reconstruction efficiencies, other offline acceptances, and background rejection power have all been extensively studied, including dependencies on counting rates in the detector. These studies have led to the careful and conservative estimates of the proposed sensitivity increases. These improvements are based on modest and well understood incremental upgrades to the beam delivery and detector systems.

The background levels have already been well established by E787 to be small enough not to contribute significantly to the determination of $|V_{td}|$ by E949. The measurement of the $K^+ \to \pi^+ \nu\overline{\nu}$ branching ratio depends critically on this large and well determined background rejection power. The importance of having already demonstrated this capability can not be overstated. Equally important is the ability to accurately calculate the background level. The extensive knowledge of the detector and background sources, as measured by the sophisticated techniques of E787, provide a degree of certainty that is not normally available to a new proposal. Additional background rejection capability will be included in E949 to exploit the region below the $K_{\pi 2}$ peak and to gain further sensitivity by operating at higher rates.

The new capital investment from DOE is quite modest and is further leveraged by a large factor from in-kind contributions from international collaborators. It builds on the significant investment already made in the E787 detector and beam line and takes advantage of the most intense proton synchrotron in the world, by using an idled AGS when it is not injecting for RHIC. The modest and well understood upgrades give an increased sensitivity per hour of 6–14 times that of the published E787 result from 1995 data.

The tantalizing prospect of new physics, based on the apparently large branching ratio observed by E787, requires follow-up. E949 will decisively resolve the issue, and if new physics is not found, will determine the elusive CKM matrix element $|V_{td}|$. The origin of CP-violation is one of the most important outstanding issues in the Standard Model. Determination of CP-violation parameters from the K system is critical to this understanding and the measurement of B($K^+ \to \pi^+ \nu\overline{\nu}$) is one of the cleanest ways for advancing this, through determination of $|V_{td}|$.

Appendices

A Other Physics

In addition to the main mode of interest, $K^+ \to \pi^+ \nu\overline{\nu}$, other K^+ decay processes, many of great interest to tests of low-energy QCD models such as chiral perturbation theory (CHPT) [65], can be studied in E949. These include $K^+ \to \pi^+ \mu^+ \mu^-$, $K^+ \to \pi^+ \gamma\gamma$, $K^+ \to \pi^+ \pi^\circ \gamma$, $K^+ \to e^+ \nu \mu^+ \mu^-$, $K^+ \to \mu^+ \nu_\mu \gamma$, $K^+ \to \pi^+ \gamma$, $K^+ \to \pi^+ X^\circ$, $K^+ \to \pi^\circ \mu^+ \nu_\mu \gamma$ and $K^+ \to \pi^+ \pi^\circ$:$\pi^\circ \to \nu\overline{\nu}$.

CHPT provides a systematic method to analyze kaon decays in which perturbative QCD is not applicable. It uses only the symmetries of the Standard Model, and the 8 lightest pseudoscalar mesons, π, K, $\bar{K}$, and η, are assumed to be the Nambu-Goldstone bosons due to the spontaneously broken axial $SU(3)$ symmetry. A low-energy effective Lagrangian is obtained by expanding the most general chiral Lagrangian in powers of external momenta of the pseudoscalar mesons.

Calculations of order $p^4 \sim p^6$ in the momentum expansion are the present state of the art. Systematic studies of 'medium-rare' K decays are one of the most stringent tests for the theory as they are sensitive to terms of the order of p^4 and p^6.

A.1 Results from E787

In addition to the first observation of $K^+ \to \pi^+ \nu\overline{\nu}$, E787 reported the first observation of the decay $K^+ \to \pi^+ \gamma\gamma$ [66]. The branching ratio and invariant mass $M_{\gamma\gamma}$ for the decay $K^+ \to \pi^+ \gamma\gamma$ are predicted by CHPT [68–72]. The prediction for $M_{\gamma\gamma}$ is striking. Instead of a smooth phase space distribution, there is a sharp turn-on above $M_{\gamma\gamma} = 2M_\pi$ due to a dominant pion-loop contribution. The measured spectrum verifies this prediction, as can be seen from the momentum spectrum of the π^+ shown in figure 23. The $K^+ \to \pi^+ \gamma\gamma$ trigger had two components: one accepting events with a P_π above

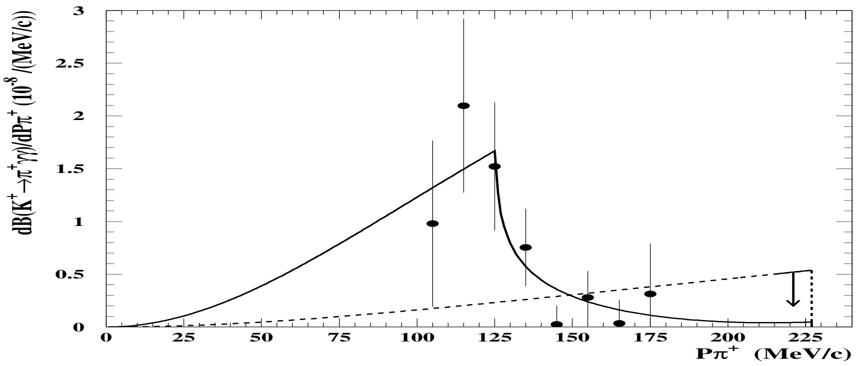

Figure 23: $K^+ \to \pi^+ \gamma\gamma$: 31 events. The solid line is the best CHPT fit. The dashed line is a phase-space distribution normalized to the 90%CL limit in the $\pi\gamma\gamma1$ region.

the $K_{\pi 2}$ peak ($\pi\gamma\gamma 1$) and one accepting P_π below the $K_{\pi 2}$ peak ($\pi\gamma\gamma 2$). There were 31 events observed in the $\pi\gamma\gamma 2$ sample and none observed in the $\pi\gamma\gamma 1$ sample. The model independent branching ratio is

$$B(K^+ \to \pi^+ \gamma\gamma \ : 100 < P_{\pi^+} < 180\mathrm{MeV/c}) = (6.0 \pm 1.5 \pm 0.7) \times 10^{-7}. \qquad (1)$$

The fit to the branching ratio and spectrum favors the CHPT parameter of $\hat{c} = 1.8 \pm 0.6$ with the so called 'unitarity corrections' of the order of p^6 [73,74]. The total branching ratio (assuming $\hat{c}$=1.8) is

$$B(K^+ \to \pi^+ \gamma\gamma \ ) = (1.1 \pm 0.3 \pm 0.1) \times 10^{-6}. \qquad (2)$$

In the $\pi\gamma\gamma 1$ region a 90%CL limit of

$$B(K^+ \to \pi^+ \gamma\gamma \ : P_{\pi^+} > 215\mathrm{MeV/c}) < 6.1 \times 10^{-8} \qquad (3)$$

was set.

E787 also reported the first observation of the decay $K^+ \to \pi^+ \mu^+ \mu^-$ [67]. Two separate analyses of this decay were made. In the first, all three tracks were fully reconstructed. In the second, the minimum requirement for the third track was that its energy was measured. In the first analysis a total of 10.6±4.7 events were observed and in the second analysis 196.0±16.7 events were observed (see figure 24). These

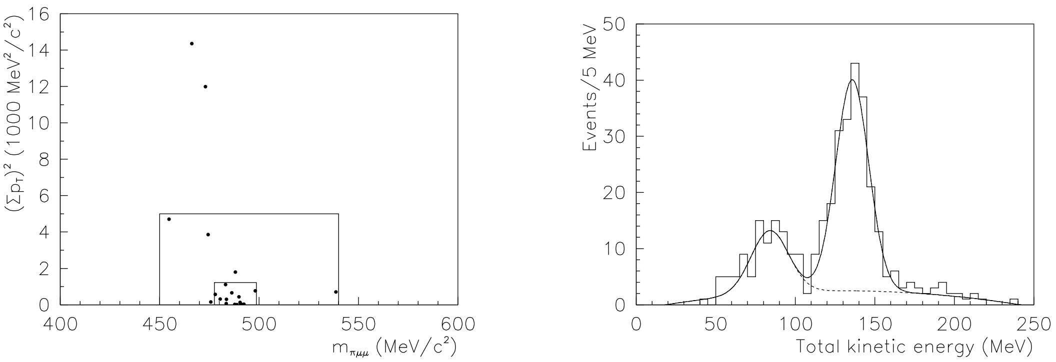

Figure 24: Final event candidates for $K^+ \to \pi^+ \mu^+ \mu^-$: a) 3-track events and b) 2-track events.

two analyses were combined to give a branching ratio for this decay of:

$$B(K^+ \to \pi^+ \mu^+ \mu^- \ ) = (5.0 \pm 0.4^{stat} \pm 0.7^{syst} \pm 0.6^{theor}) \times 10^{-8}. \qquad (4)$$

This branching ratio implies a value for the CHPT parameter [75] $w_+ = 1.07 \pm 0.07$. This value is larger than that derived from $K^+ \to \pi^+ e^+ e^-$: $w_+ = 0.89^{+0.24}_{-0.14}$ by the BNL E777 experiment [76].

Using the same data set, a search for the decay $K^+ \to e^+ \nu \mu^+ \mu^-$ was made. In this decay mode, the structure dependent terms dominate over inner bremsstrahlung due to helicity suppression. No events were observed and the 90% CL upper limit of the branching ratio was established to be 5×10^{-7} [77]. This result is consistent with a CHPT prediction of 1.1×10^{-8}.

An engineering run in 1994 produced another discovery: the first observation of the Structure Dependent (SD$^+$) component of the radiative decay $K^+ \to \mu^+\nu_\mu\gamma$ [78,79]. The $K^+ \to \mu^+\nu_\mu\gamma$ ($K_{\mu 2\gamma}$) decay is dominated by Inner Bremsstrahlung (IB), which has been well measured [80]; however, the structure dependent component had not previously been seen. Two days of data taking with a special trigger, selecting a high energy muon accompanied by a high energy photon, yielded a total of $\sim$2700 $K_{\mu 2\gamma}$ events with a background of 100 events ($K_{\mu 3}$ and $K_{\pi 2}$ with a missing photon and $K_{\mu 2}$ with an accidental photon). Of the 2700 $K_{\mu 2\gamma}$ events a clear signal of $\sim$900 events from the SD$^+$ component is seen in figure 25. From a more sophisticated

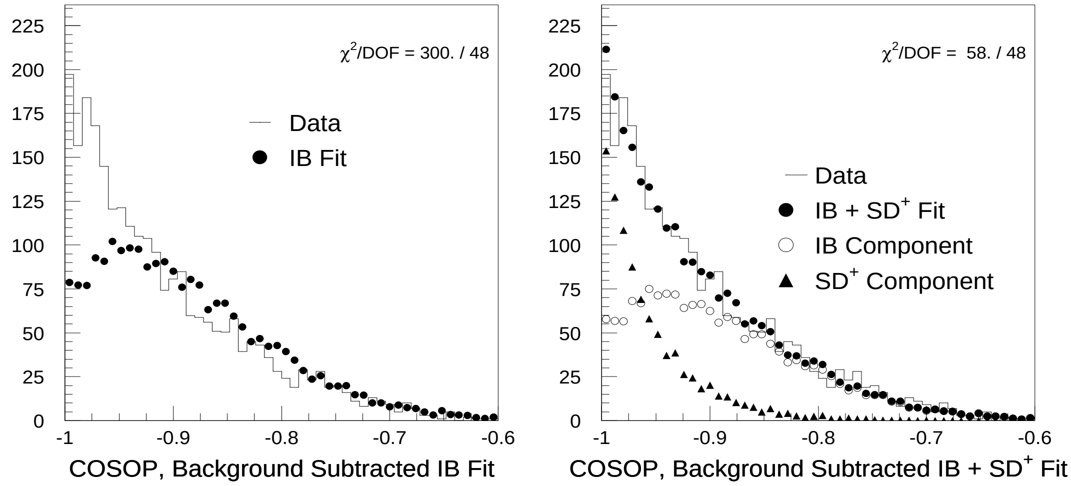

Figure 25: Distribution of $\cos\theta_{\mu\gamma}$ for E787 $K^+ \to \mu^+\nu_\mu\gamma$ candidates. A fit to IB alone is shown in (a), and a fit to both IB and SD$^+$ is shown in (b).

analysis, fitting E_{μ^+} and E_γ to IB, SD$^\pm$ and the interference terms, the branching ratio for the SD$^+$ decay is:

$$B(\mathrm{SD}^+\ ) = (1.33 \pm 0.12 \pm 0.18) \times 10^{-5} \tag{5}$$

and the form factor $|F_V + F_A| = 0.165 \pm 0.007 \pm 0.011$. This can be compared to the $O(p^4)$ CHPT calculation of $F_V + F_A = -0.137 \pm 0.006$ and B(SD$^+$)=9.22×10^{-6} (Ref [81]). An $O(p^6)$ calculation is underway [82,83].

A.2 E787/E949 Prospects

In 1995, a trigger was implemented to observe $K^+ \to \pi^+\pi^\circ\gamma$. This decay is a sum of the dominant Inner Bremsstrahlung (IB) contribution and the smaller direct emission (DE) contribution of $O(p^4)$ which is due to the chiral $U(1)$ anomaly. Measurements of the DE contribution by previous experiments disagree with the prediction of CHPT by about a factor two, although errors on both experiment and theory are large [84]. E787 should observe $\sim$20,000 (IB+DE) events. This will be enough to settle the outstanding issues in this decay.

In 1998, a trigger was implemented to search for the decay $K^+ \to \pi^\circ\mu^+\nu_\mu\gamma$. This decay, which has never been observed, is predicted to occur with a branching ratio of

1.9×10^{-5}. This decay is sensitive to the L9 and L10 coefficients, and the anomalous amplitude of CHPT[85]. In addition, in this decay it is possible to search for a CP-violating T-odd correlation of the three observed final state momenta[86]. Such an effect can show up in the interference between the inner bremsstrahlung and the direct emission components of the decay. Since it is not necessary to measure the muon polarization, E787/E949 may be able to do quite a reasonable job.

With the same trigger, a search for the decay $K^+ \to \pi^\circ \pi^\circ \mu^+ \nu_\mu$, which has never been observed, will proceed. The measurement of $K^+ \to \pi^+ \pi^\circ \gamma$ will be also improved in the low π^+ momentum region, which may result in a discovery of the CP violating interference of IB with the E1 transition.

In addition to the CHPT decay modes, E787/E949 is capable of searching for yet more exotic modes such as $K^+ \to \pi^+ \gamma$, $K^+ \to \pi^+ X^\circ$; $X^\circ \to \gamma\gamma$ (X° : new light neutrals) [66], and $K^+ \to \pi^+ \pi^\circ$:$\pi^\circ \to \nu \overline{\nu}$ [87].

B History of E787

A proposal to search for the process $K^+ \to \pi^+ \nu\overline{\nu}$ [4] and related decays was submitted to the AGS Program Committee in October of 1983 by a collaboration of BNL, Princeton, and the TRIUMF laboratory of Canada. The main object was to observe $K^+ \to \pi^+ \nu\overline{\nu}$ at the Standard Model-predicted level unless new physics intervened. The proposal was promptly approved, initiating Experiment 787. The collaboration spent the next year in R&D and design studies culminating in a technical design. First funding was obtained in October of 1984 and construction began in January, 1985. A test run with a partial detector was conducted in 1987. Construction was completed in January of 1988 and the experiment was ready for an engineering and commissioning run in February of that year. In addition, two weeks of physics-quality data were taken. These data resulted in four publications in Physical Review Letters: an improvement in the previous limit on $K^+ \to \pi^+ \nu\overline{\nu}$ by a factor ~ 4, and order of magnitude improved limits on the processes $K^+ \to \pi^+ \gamma\gamma$, $K^+ \to \pi^+ \mu^+ \mu^-$, $\pi^\circ \to \nu\overline{\nu}$ and the first-ever limit on $K^+ \to \mu^+ \nu \mu^+ \mu^-$.

The first major data collecting run took place the following March (1989). Publications based on that data included a further improved limit on $K^+ \to \pi^+ \nu\overline{\nu}$ (by a factor ~ 7), and the first-ever limit on the class of processes $\pi^\circ \to \gamma X^\circ$ (where X° is an unobserved neutral particle or system of particles).

Two more major data collection runs took place in 1990 and 1991. These resulted in the discovery of $K^+ \to \pi^+ \gamma\gamma$ and of $K^+ \to \pi^+ \mu^+ \mu^-$, and a further improvement on the limit of on $K^+ \to \pi^+ \nu\overline{\nu}$, to a 90%c.l. upper limit of 2.4×10^{-9}. This was a ~ 60-fold improvement on the sensitivity available before the experiment began, and was actually within the range of theoretical prediction for this process current at the inception of the experiment. However in the ensuing years, the prediction had fallen into the range $(0.6 - 6) \times 10^{-10}$.

The collaboration wished to pursue this process down to the predicted level, but it had become clear, even by the time of the first major data run that neither the beam nor the detector was capable of this. Moreover the AGS was not capable of producing sufficient protons. Fortunately a major upgrade of the AGS intensity was scheduled. Thus a proposal for a major detector and beamline upgrade was submitted. This was approved in November of 1989, and R&D was conducted in parallel with the 1989-91 run. Several institutions from Japan (INS-Tokyo, KEK, and later Osaka and Fukui Universities) joined the collaboration in 1992 under the Japan-U.S.A. Cooperative Research and Development Project and participated in the detector upgrade. Fabrication of a new beamline began in August of 1990 and was complete by May of 1992. The new beam was doubly separated and could produce a positive beam in which the $K/(\pi + \mu)$ ratio was as high as $5:1$. This is in contrast to the previous beam where this ratio was typically $1:3$. The new beam also had an acceptance roughly twice that of its predecessor. It was first used for prototype testing for the new detector systems. The detector upgrade, in which 80% of the systems were replaced or highly modified, was largely complete in time for the commissioning run

[4] Then known to be $< 10^{-7}$

of May, 1994. Data collected during that run led to the first observation of structure dependent radiation in the process $K_{\mu 2\gamma}$.

The first full data run of the upgraded experiment took place in 1995. There was nearly a five-fold increase in the rate of collecting sensitivity to $K^+\to\pi^+\nu\overline{\nu}$. This run yielded the first example of $K^+\to\pi^+\nu\overline{\nu}$. Subsequent runs were taken in 1996, 1997 and 1998. The sensitivity collected in total is expected to be in the range (7–10)$\times 10^{-11}$/event.

E787 has produced many results in addition to the ones mentioned above. Table 4 lists all those which have so far been made public. In addition, several other analyses are in progress.

Mode	Result	Gain w.r.t. prev. data	Comments
$K^+\to\pi^+X^\circ$	$< 3\times 10^{-10}$	127	new particle search; future: find/rule out f°
$K^+\to\pi^+\nu\overline{\nu}$	$(4.2^{+9.7}_{-3.5})\times 10^{-10}$	145	constrain new physics,$\lvert V_{td}\rvert$ **Discovery!**
$K^+\to\pi^+\mu^+\mu^-$	$(5.0\pm 1.0)\times 10^{-8}$	$4,500$	χPT study future $\overline{\rho}$ determination **Discovery!** ~ 200 events
$K^+\to\pi^+\gamma\gamma$	$(1.1\pm 0.3)\times 10^{-6}$	100	Long distance effects search for light $X^\circ\to\gamma\gamma$ **Discovery!** ~ 30 events
$K^+\to\mu^+\nu_\mu\gamma$	$(1.33\pm 0.12)\times 10^{-5}$	$1,000$	χPT study 1st observation of SD$^+$ **Discovery!** ~ 900 events
$K^+\to\mu^+\nu\mu^+\mu^-$	$< 4.1\times 10^{-7}$	$2.4M$	Higgs hunting ground; no previous limit
$K^+\to e^+\nu\mu^+\mu^-$	$< 5\times 10^{-7}$	$2.0M$	χPT study; no previous limit
$\pi^\circ\to\nu\overline{\nu}$	$< 8\times 10^{-7}$	10	Also search for new light particles
$\pi^\circ\to\gamma X^\circ$	$< 5.3\times 10^{-4}$	$1,900$	New light vectors no previous limit

Table 4: E787 results.

A list of the major publications from E787 is provided in Table 5.

References

[1] M.K. Gaillard and B.W. Lee, Phys. Rev. D **10**, 897 (1974).

[2] T. Inami and C. S. Lim, Prog. Theor. Phys. **65**, 297 (1981).

M.S. Atiya *et al.*, Phys.Rev.Lett. **63**, 2177–2180 (1989).
M.S. Atiya *et al.*, Phys.Rev.Lett. **64**, 21–24 (1990).
M.S. Atiya *et al.*, Phys.Rev.Lett. **65**, 1188–1191 (1990).
M.S. Atiya *et al.*, Phys.Rev.Lett. **66**, 2189–2192 (1991).
M.S. Atiya *et al.*, Phys.Rev.Lett. **69**, 733–736 (1992).
M.S. Atiya *et al.*, Nucl.Phys. **A527**, 727c–729c (1991).
M.S. Atiya *et al.*, Phys.Rev.Lett. **70**, 2521–2524 (1993).
M.S. Atiya *et al.*, Phys.Rev. **D48**, 1–4 (1993).
S. Adler *et al.*, Phys.Rev.Lett. **76**, 1421–1424 (1996).
S. Adler *et al.*, Phys.Rev.Lett. **79**, 2204–2207 (1997).
P. Kitching *et al.*, Phys.Rev.Lett. **79**, 4079–4082 (1997).
S. Adler *et al.*, Phys.Rev.Lett. **79**, 4756–4759 (1997).
M.S. Atiya *et al.*, IEEE Trans.Nucl.Sci. **NS–36**, 813–817 (1989).
M.S. Atiya *et al.*, NIM **A279**, 180–185 (1989).
M.S. Atiya *et al.*, NIM **A321**, 129–151 (1992).
M. Burke *et al.*, IEEE Trans.Nucl.Sci. **NS–41**, 131 (1994).
M. Kobayashi *et al.*, NIM **A337**, 355–361 (1994).
I.-H. Chiang *et al.*, IEEE Trans.Nucl.Sci. **NS–42**, 394–400 (1995).
D.A. Bryman *et al.*, NIM **A396**, 394–404 (1997).
E.W. Blackmore *et al.*, NIM **A404**, 295–304 (1998).
T.K. Komatsubara *et al.*, NIM**A404**, 315–326 (1998).
S. Adler *et al.*, Phys.Rev. **D58**, 012003 (1998).

Table 5: Major Publications from AGS experiment E787.

[3] A.J. Buras and R. Fleischer, *Heavy Flavours II*, ed. Buras and Linder, p65 (World Scientific,1998).

[4] G. Buchalla and A.J. Buras, Nucl. Phys. **B412**, 106 (1994).

[5] M. Misiak and J. Urban, TUM-HEP-33698, IFT-14/98, hep-ph/9901278 (1998).

[6] G. Buchalla and A.J. Buras, CERN-TH/98-369, hep-ph/9901288 (1998).

[7] W.J. Marciano and Z. Parsa, Phys. Rev. **D53**, R1 (1996).

[8] G. Buchalla and A.J. Buras, Phys. Rev. **D57**, 216 (1998).

[9] J.S. Hagelin and L.S. Littenberg, Prog. Part. Nucl. Phys. **23**, 1 (1989).

[10] D. Rein and L.M. Sehgal, Phys. Rev. **D39**, 3325 (1989).

[11] M. Lu and M.B. Wise, Phys. Lett. **B324**, 461 (1994).

[12] C.Q. Geng *et al.*, Phys. Lett. **B355**, 569 (1995).

[13] S. Faijfer, Nuovo. Cim. **110A**, 397 (1997).

[14] I.I. Bigi and F. Gabbiani, Nucl. Phys. **B367**, 3 (1991).

[15] T. Hattori, T. Hasuike, and S. Wakaizumi, hep-ph/9804412, TOKUSHIMA-98-01, Apr 1998.

[16] K. Agashe and M. Graesser, Phys. Rev. D **54**, 4445 (1996).

[17] M. Leurer, Phys. Rev. Lett. **71**, 1324 (1993).

[18] S. Davidson, D. Bailey, and B. Campbell, Z. Phys. **C61**, 613 (1994).

[19] Y. Kiyo *et al.*, HUPD-9823, GATC-98-1, hep-ph/9809333 (1998).

[20] Z. Xiao, L. L ü, H. Guo and G. Lu, hep-ph/9903347 (1998).

[21] Z. Xiao, C. Li and K. Chao, hep-ph/9903348 (1998).

[22] A.J. Buras, A. Romanino, and L.Silvestrini, Nucl. Phys. **B520**, 3 (1998).

[23] G-C. Cho, hep-ph/9804327, KEK-TH-568, Apr 1998; G-C. Cho, Eur. Phys. J. **C5**, 525 (1998).

[24] T. Goto, Y. Okada, and Y. Shimizu, Phys. Rev. **D58**, 094006 (1998), hep-ph/9804294.

[25] Y. Grossman and Y. Nir, Phys. Lett. **B398**, 163 (1997).

[26] G. Couture and H. König, Z. Phys. **C69**, 167 (1996).

[27] G. Colangelo and G. Isidori, JHEP-9809-009, hep-ph/9808487 (1998).

[28] G. Buchalla and A.J. Buras, TUM-HEP-334/98, hep-ph/9811471 (1998).

[29] G. Isidori, hep-ph/9902235 (1999).

[30] D. Silverman, Phys. Rev. **D58**, 095006 (1998).

[31] T. Barakat, CV-HEP/98-03, hep-ph/9807317 (1998).

[32] M.B. Popovic and E. Simmons, Phys. Rev. **D58**, 095007 (1998).

[33] B. Winstein, private communication.

[34] A.J. Buras and L.Silvestrini, TUM-HEP-334/98, hep-ph/9811471 (Nov. 1998).

[35] A. Buras, private communication.

[36] G. Buchalla *et al.*, Rev. Mod. Phys. **68**, 1125 (1996).

[37] S. Adler *et al.*, Phys. Rev. Lett. **79**, 2204 (1997).

[38] M.S. Atiya *et al.*, Phys. Rev. **D48**, R1 (1993).

[39] G.D. Cable, A Search for the Reaction $K^+ \rightarrow \pi^+ \nu\overline{\nu}$, Ph.D. Thesis at the University of Chicago, EFI-73-19 (1973).

[40] M.S. Atiya *et al.*, NIM **A321**, 129 (1992).

[41] I.-H. Chiang *et al.*, to be submitted to NIM **A**.

[42] E.W. Blackmore *et al.*, NIM **A404**, 295 (1998).

[43] M.S. Atiya *et al.*, NIM **A279**, 180 (1989).

[44] I.-H. Chiang *et al.*, IEEE Trans. Nucl. Sci. **NS–42**, 394 (1995).

[45] T.K. Komatsubara *et al.*, NIM **A404**, 315 (1998).

[46] M. Kobayashi *et al.*, NIM **A337**, 355 (1994).

[47] D.A. Bryman *et al.*, NIM **A396**, 394 (1997).

[48] M. Burke *et al.*, IEEE Trans. Nucl. Sci. **NS–41**, 131 (1994).

[49] C. Witzig and S. Adler, Real-Time Comput. Appl., 123 (1993).

[50] S.S. Adler, Inter. Conf. Electr. Part. Phys., 133 (1997).

[51] C. Zein *et al.*, Real-Time Comput. Appl., 103 (1993).

[52] S.S. Adler *et al.*, to be submitted to IEEE.

[53] J.M. Brennan and T. Roser, *'High intensity performance of the Brookhaven AGS'*, 5^{th} Europ.Part.Acc.Conf.(EPAC96), 530 (1996).

[54] J. Sandberg and T. Roser, private communication.

[55] P. Pile and I-H. Chiang, private communication.

[56] M.S. Atiya *et al.*, Phys. Rev. Lett. **64**, 21 (1990).

[57] M.S. Atiya *et al.*, Nucl. Phys. **A527**, 727c (1991).

[58] M.S. Atiya *et al.*, Phys. Rev. Lett. **70**, 2521 (1993).

[59] S. Adler *et al.*, Phys. Rev. Lett. **76**, 1421 (1996).

[60] Y. Asano *et al.*,Phys. Lett. **107B**, 159 (1981).

[61] G.D. Cable *et al.*,Phys. Rev. **D8**, 3807 (1973).

[62] J.H. Klems *et al.*,Phys. Rev. **D4**, 66 (1971).

[63] A.J. Buras, hep-ph/9806471, TUM-HEP-316-98, June 1998.

[64] C. Bernard, hep-ph/9709460, July 1997.

[65] J.F. Donoghue, E. Golowhich, and B.R. Holstein, *Dynamics of the Standard Model*, (Cambridge University Press, Cambridge, 1992), and references therein.

[66] P. Kitching *et al.*, Phys.Rev.Lett. **79**, 4079 (1997).

[67] S. Adler *et al.*, Phys.Rev.Lett. **79**, 4756 (1997).

[68] G. Ecker *et al.*, Nucl.Phys. **B303**, 665 (1988).

[69] G. Ecker *et al.*, Phys.Lett. **B237**, 481 (1990).

[70] H.Y. Cheng, Phys.Rev. **D42**, 72 (1990).

[71] C. Bruno and J. Prades, Z.Phys. **C57**, 585 (1993).

[72] G. Ecker *et al.*, Nucl.Phys. **B394**, 101 (1993).

[73] L. Cappiello *et al.*, Phys.Lett. **B298**, 423 (1993).

[74] A.G. Cohen *et al.*, Phys.Lett. **B304**, 347 (1993).

[75] G. Ecker *et al.*, Nucl.Phys. **B291**, 692 (1987).

[76] C. Alliegro *et al.*, Phys.Rev.Lett. **68**, 278 (1992).

[77] S. Adler *et al.*, Phys. Rev.**D58** 012003 (1998).

[78] M. Convery, Proceedings of DPF96, The Minneapolis Meeting, 1015 (1998).

[79] M. Convery, *First Measurement of Structure Dependent* $K^+ \to \mu^+ \nu_\mu \gamma$, Princeton University PhD. thesis (1996).

[80] Y. Akiba *et al.*, Phys.Rev. **D32**, 2911 (1985).

[81] J. Bijnens *et al.*, Nucl.Phys. **B396**, 81 (1993).

[82] J. Bijnens and P. Talavera, Nucl.Phys. **B489**, 387 (1997).

[83] L. Ametller *et al.*, Phys.Lett. **B303**, 140 (1993).

[84] G. Ecker, *et. al.*, *Phys. Lett.*,**B278** 337 (1992).

[85] B.R. Holstein, *Phys. Rev*,**D41** 2829 (1990).

[86] J.L. Gervais, *et. al*,, *Phys.Lett.*, **20** 432 (1966).

[87] M.S. Atiya *et al.*, Phys.Rev.Lett. **66**, 2189 (1991).